
Diet is correlated with otolith shape in marine fish

Mille Tiphaine ^{1,*}, Mahe Kelig ¹, Cachera Marie ², Villanueva Ching-Maria ³, De Pontual Helene ³,
Ernande Bruno ¹

¹ Ifremer, Centre Manche Mer du Nord, Laboratoire ressources halieutiques, BP 699, 62321 Boulogne-sur-mer, France

² Laboratoire des Sciences de l'Environnement Marin, UMR 6539, Institut Universitaire Européen de la Mer, 29280 Plouzané, France

³ IFREMER, Centre de Bretagne, Unité Sciences et Technologies Halieutiques, Z.I. Pointe du Diable, CS10070, 29280 Plouzané, France

* Corresponding author : Tiphaine Mille, email address : tiphaine.mille@ifremer.fr

Abstract :

Previous studies have shown that food amount influence fish otolith structure, opacity and shape and that diet composition has an effect on otolith chemical composition. This study investigated the potential correlation between diet and otolith shape in 5 wild marine fish species by addressing 4 complementary questions. First, is there a global relationship between diet and otolith shape? Second, which prey categories are involved in this relationship? Third, what are the respective contributions of food quantity and relative composition to diet–otolith shape co-variation? Fourth, is diet energetic composition related to otolith shape? For each species, we investigated how otolith shape varies with diet. These questions were tackled by describing diet in the analysis in 4 different ways, while also including individual-state variables to remove potential confounding effects. First, besides the strong effect of individual-state, a global relationship between diet and otolith shape was detected for 4 out of 5 fish species. Second, both main and secondary prey categories were related to variability in otolith shape. Otolith outline reconstructions revealed that both otolith global shape and its finer details co-varied with these prey categories. Third, the contribution of relative diet composition to diet–otolith shape co-variation was much higher than that of ingested food quantity. Fourth, the energetic composition of diet was related to otolith shape of only one species. These results suggest that diet in marine fish species may influence the quantity and composition of saccular endolymph proteins which play an important role in otolith biomineralization and their resulting 3D structure.

Keywords : Elliptic Fourier analysis, English Channel, Interspecific, Morphometric analysis, Otolith growth, Saccular otolith, Stomach contents

49 **Introduction**

50 Otoliths are calcified structures found in the inner ear of teleostean fish. They are organised
51 into 3 pairs and assist with auditory and balance functions of fish. They are critical tools in
52 fisheries science and management. Their structure allows aging individual fish and determining
53 population age structure for stock assessment (e.g. Worthington et al. 1995, Caldow &
54 Wellington 2003). Their morphology can be used for individual assignment to (sub-
55)populations and to infer population structure (e.g. Castonguay et al. 1991, Stransky et al. 2008).
56 The *sagittae* (the most studied otolith pair because of their large size) are mainly composed of
57 calcium carbonate in aragonite form deposited on an organic matrix which represents 0.1 to
58 10% of total material (Degens et al. 1969). The organic matrix, although present in minute
59 amounts in otoliths, is thought to play a key role in its formation as in all biomineralization
60 processes (Nagasawa 2013). Biomineralization of the sagittal otolith (referred to as “otolith”
61 hereafter) is an acellular process that takes place in the saccule (otic sac). Otoliths grow by
62 accretion and precipitation of organic and ionic precursors contained in the saccular endolymph
63 in which they are bathing. Otolith biomineralization is therefore totally dependent on the
64 endolymph composition and precursors that are either synthesized (organic) or transported
65 (ionic) by secretory cells and ionocytes, respectively, belonging to the saccular epithelium
66 (Payan et al. 2004). Moreover, the spatial distribution of these cells in the saccular epithelium
67 induces concentration gradients of both ions and organic precursors in the endolymph that are
68 involved in otolith biomineralization processes (Pisam et al. 1998, Payan et al. 1999, Borelli et
69 al. 2001).

70 Otolith biomineralization results from multi-causal processes due to the interaction of many
71 internal (physiological) and external (environmental) factors (Allemand et al. 2007), which
72 generates high morphological variability in otolith shape at both intra- and inter-specific level.

73 First, otolith shape is species-specific (Tuset et al. 2006), reflecting genetic determinism
74 (L'Abée-Lund 1988, Vignon & Morat 2010).

75 Second, factors or processes acting on fish metabolism and physiology have an impact on
76 otolith morphology, such as ontogenetic development (size: Hüsey, 2008 and age: Castonguay
77 et al. 1991, sexual maturation (Mérigot et al. 2007) or sex (Castonguay et al. 1991, Bolles &
78 Begg 2000). Third, environmental factors such as water temperature produce otolith growth
79 variation and thus shape variability (Cardinale et al. 2004). Food quantity can also impacts
80 otolith shape both directly and indirectly. It has an indirect effect on global otolith shape through
81 its effect on otolith growth and a direct effect on otolith crenation (Gagliano & McCormick
82 2004, Cardinale et al. 2004, Hüsey 2008).

83 Consequences of fish nutrition on otolith structure and growth, especially the impact of
84 starvation or food restriction and satiation, have been well studied (Molony & Choat 1990,
85 Molony & Sheaves 1998, Hüsey & Mosegaard 2004, Fernandez-Jover & Sanchez-Jerez 2015).

86 A decrease in the otolith increments' width and thus in otolith growth was observed after
87 reduced feeding periods (Massou et al. 2002). More translucent otolith material is deposited in
88 response to severe (long period and low ration) food restriction, which can lead to otolith
89 structural discontinuities that do not conform to the seasonal opaque and translucent layers of
90 annuli (Høie et al. 2008), referred to as "checks" (Panfili et al. 2002). Such changes in opacity
91 are the consequences of variation in the composition of inorganic and organic otolith
92 compounds (Jolivet et al. 2013) and precursors. A starvation period leads to change in blood
93 plasma composition, which generates a decrease in the acid-base equilibrium in the saccular
94 endolymph and thus, induces a reduction of aragonite precipitation rate. As a consequence, a
95 reduction of daily growth rate due to starvation could be observed even if calcium concentration
96 was not affected (Payan et al. 1998). Concerning the organic precursors, only the protein
97 «Factor Retarding Crystallization» (FRC) concentration decreases during starvation periods

98 especially in the proximal zone (Guibbolini et al. 2006). This change may play a key role in the
99 intensity of aragonite deposition and thus otolith growth. In conclusion, food amounts may
100 affect otolith growth, opacity (or structure) and biomineralization.

101 Several papers have also documented a link between energy metabolism and otolith growth.
102 Otolith growth is closely related to standard metabolic rate (Mosegaard et al. 1988, Fablet et al.
103 2011) and otolith accretion appears regulated by feeding-induced thermogenesis (Huuskonen
104 & Karjalainen 1998). Otolith growth in larvae and juveniles is also related to individuals'
105 condition index estimated from fish lipid composition (Amara et al. 2007), which in turn
106 depends on zooplankton biomass (Suthers et al. 1992). Besides the fact that lipid quantity such
107 as triacylglycerol content can be used as a condition index for fish (Fraser 1989), taken together
108 these results suggest that lipid content in diet and energy metabolism may influence otolith
109 growth. Given that lipid content of prey is the primary determinant of their energy density
110 (Anthony et al. 2000, Spitz et al. 2010), diet energy content or composition in terms of energetic
111 prey categories is a good candidate for encompassing both effects.

112 Along with food abundance and energy content, diet composition can also affect otoliths,
113 especially their chemical composition (Sanchez-Jerez et al. 2002). For instance, Barium (Ba)
114 and strontium (Sr) concentrations in *Pomatomus saltatrix* otoliths were related to the
115 concentration of these elements in their prey (Buckel et al. 2004). Here, the authors assumed
116 the diet effect on Ba and Sr concentration in otoliths could be either direct or indirect through
117 diet-based growth rate changes that induce element incorporation rate variation in otoliths. Even
118 if around 80% of Sr and Ba in otoliths come from water (Walther & Thorrold 2006) and not
119 from diet, a trophic transfer may be considered as a potential source of element accumulation
120 in fish otolith. The concentration of manganese (Mn) in the habitat and prey items was also
121 related to its accumulation in otoliths (Sanchez-Jerez et al. 2002). The fact that the Mn:Ca ratio
122 in otoliths is not correlated to the same ratio in water suggests a trophic transfer of metallic

123 elements, such as Mn (Thorrold et al. 1997). Moreover, variations in $\delta^{13}\text{C}$ otolith values were
124 observed to correlate with variations in muscular $\delta^{13}\text{C}$ values among diet treatment (Elsdon et
125 al. 2010).

126 In summary, previous experimental work revealed that the food ration level affects otolith
127 structure, opacity and shape. Laboratory and wild conditions studies have shown that energy
128 metabolism and food energy content influences otolith growth and that diet composition
129 impacts otolith chemical composition. In the present study, we investigated the potential
130 relationship between diet, described as a combination of both food composition and quantity,
131 and the otolith shape at the intra-population level in five marine fish species, including three
132 roundfishes and two flatfish sampled in the wild. More specifically, we addressed four related
133 questions. We first tested for a global relationship between diet (represented by the weight of
134 each taxonomic prey category) and otolith shape. Second, in case of significant diet effect,
135 taxonomic prey categories involved in the relationship with otolith shape were identified. Third,
136 we quantified the respective contributions of food quantity and taxonomic composition to diet-
137 otolith shape co-variation. Fourth, we tested for the relationship between diet composition in
138 terms of energetic prey categories and otolith shape. For all questions, the effect of potential
139 confounding factors, i.e. individual-state variables (age, length, sex and maturity status), on
140 otolith shape was quantified and removed to obtain unbiased estimates of food effects.

141

142 **Materials and methods**

143 **Sample collection**

144 Five marine fish, three roundfishes and two dextral flatfishes, were sampled in the eastern
145 English Channel (Fig. 1) : 47 striped red mullets (*Mullus surmuletus*), 28 tub gurnards
146 (*Chelidonichthys lucerna*), 32 red gurnards (*Chelidonichthys cuculus*) and 42 European plaices
147 (*Pleuronectes platessa*) and 36 common soles (*Solea solea*) (Table 1). These species were

148 chosen because of their commercial interest, of their large sample size, they represent a
149 combination of round and flat fish, and they are among the most abundant ones in the area. For
150 each species, individuals sampled belonged to a single population for each species. All fish
151 were caught during the annual Channel Ground Fish Survey (CGFS) operated on board the R.V.
152 “Gwen Drez” in October 2009. The fishing gear was a Grande Ouverture Verticale bottom trawl
153 with a 10-mm stretched mesh size in the codend, that was towed for 30 min at an average speed
154 of 3.5 knot (Coppin et al. 2002). Following their capture, fish were identified at the specific
155 level and sampled individuals were frozen in liquid nitrogen for their conservation on board.
156 Back in the laboratory, individuals were defrosted, measured (total length, L_T) to the nearest
157 centimeter and their sex and maturity status were determined by gonads macroscopic
158 observation according to the recommendations of international expert groups (ICES 2014). The
159 digestive tract was extracted and its contents removed and stored in a Petri-dish for analysis.
160 Sagittal otoliths were also removed from each individual, one of them being used to estimate
161 the individual’s age by interpreting macrostructures according to accepted standard ageing
162 protocols (ICES 2010, 2012) and the second one for shape analysis, each of them coming
163 always from the same side (Table 1). For striped red mullet, age was estimated by reading
164 macrostructures on the sagittal otolith pair. The left otolith was read under transmitted light
165 while the right one was read under reflected light before being burned to confirm the age
166 estimation done previously (ICES 2012). The left otolith (not burned) was then used for shape
167 analysis. Even though recommendations from ICES expert groups do not exist for tub and red
168 gurnards, the same methods were effective when applied to these species. For European plaice,
169 the entire left otolith was used to estimate age as well as for shape analysis (ICES 2010),
170 whereas, for common sole, a transversal section of the left otolith was necessary for age reading
171 (Mahé et al. 2012) so that the right otolith was used for shape analysis.

172 Hereafter, we describe otolith shape analysis, diet analysis and statistical analyses as they were
173 conducted for each species separately.

174

175 **Otolith shape analysis**

176 Each otolith was cleaned by an ultrasonic bath in water at room temperature for a duration of
177 10 minutes, then brushed to remove residual tissues and stored dry in tubes. Batches of otoliths
178 were automatically digitized using orthogonal projection at a high resolution (3200 dpi) using
179 a scanner EPSON V750 and individual images were extracted. An Elliptical Fourier analysis
180 was performed on each otolith contour delineated and extracted after image binarization. This
181 method reconstructs any type of shape with a closed two dimensional contour (Kuhl & Giardina
182 1982) using ellipses named harmonics. Each harmonic (H_i) is characterized by 4 coefficients
183 (A_i, B_i, C_i and D_i), called Elliptic Fourier Descriptors (EFDs), which correspond to the
184 parameters of the trigonometric equations describing the corresponding ellipse. The number of
185 harmonics n used to reconstruct each otolith outline in the sample was determined as follows
186 using the cumulated Fourier power ($P_F(n_k)$). This parameter was calculated for each otolith
187 k as the sum of the proportion of variation in contour coordinates accounted for by each
188 harmonic and it is equal to:

$$189 \quad P_F(n_k) = \sum_{i=1}^{n_k} \frac{A_i^2 + B_i^2 + C_i^2 + D_i^2}{2}. \quad (1)$$

190 The number of harmonics n_k was then chosen such that $P_F(n_k)$ reaches 99.99% of variation
191 in contour coordinates or, in other words, such that shape is reconstructed at 99.99% (Lestrel
192 2008). A majority of studies (e.g. Mérigot et al. 2007, Lestrel 2008) compute the cumulated
193 Fourier power P_F using EFDs averaged across the full sample or part of it, so that the selected
194 harmonics describe the average otolith shape. In this study, $P_F(n_k)$ and n_k were calculated for

195 each individual otolith k in order to ensure that each individual otolith in the sample was
196 reconstructed with a precision of 99.99% The maximum number of harmonics $n = \max(n_k)$
197 across all otoliths was then used to reconstruct each individual otolith of the sample.
198 After extracting the n harmonics for each individual otolith, their EFDs were normalized by
199 the first harmonic providing EFDs invariant with respect to size, rotation and starting point
200 (Kuhl & Giardina 1982), and resulting in the degeneration of the first three EFDs (A_i , B_i and
201 C_i), respectively equal to 1, ≈ 0 and ≈ 0 for each individual. EFDs were then gathered in a
202 matrix \mathbf{F} with EFDs as columns and individuals as rows.
203 All otolith images and EFDs were obtained using the software TNPC 7.0 (www.tnpc.fr).
204

205 **Diet analysis**

206 For each fish, taxonomic identification of prey items in the stomach content was carried out
207 using a binocular loupe. Prey items were identified to the lowest possible taxonomic level
208 before being weighed (g, wet weight). In view of their high diversity, preys were grouped into
209 22 taxonomic categories (Table S1 in Supplementary material) mostly based on their main
210 taxonomic level. Preys were categorized at least according to their Phylum in the taxonomic
211 hierarchy (e.g. *annelida*, *cnidaria*). If further taxonomic determination was possible, taxonomic
212 prey categories were based on Class (e.g. *cephalopoda*, *gastropoda*), Order (e.g. *amphipoda*,
213 *isopoda*) or Infra-Order (e.g. *brachyoura*, *anomoura*). Teleosts were split into two taxonomic
214 prey categories depending on their energetic value. The energy content of each fish prey (found
215 at <http://www.nutraqua.com/>) was plotted. Fish species gathered in two main groups (fat and
216 lean) separated by a threshold of 1kcal.g^{-1} .
217 Alternatively, preys were regrouped into three categories based on their energetic content
218 (low/medium/high; Table S1 and Fig. S3 in Supplementary material) estimated from
219 appropriate literature (Norrbin & Båmstedt 1984, Steimle & Terranova 1985, Dauvin &

220 Joncourt 1989, Spitz et al. 2010) and following the three energetic categories proposed by Spitz
221 et al. 2010.

222 For each studied species, stomach content data were grouped in a diet composition matrix in
223 terms of weight, based either on taxonomic \mathbf{W}_t or energetic prey categories \mathbf{W}_e , with each
224 cell corresponding to the weight $w_{t,ij}$ or $w_{e,ij}$ of prey category j (columns) in the digestive
225 tract of individual i (rows). In addition, the relative contribution of taxonomic prey categories
226 to diet composition by weight ($\%W_{t,j} = \sum_i w_{t,ij} / \sum_i \sum_{j'} w_{t,ij'}$) and the relative frequency of
227 occurrence ($\%F_{t,j}$) of each taxonomic prey category (Godfriaux 1969), were computed for
228 each studied species (Fig.2).

229

230 **Statistical analyses**

231 A principal component analysis (PCA) combined with broken stick principal component
232 selection (Borcard et al. 2011, Chapter 5) was performed on the EFDs matrix \mathbf{F} . The aim was
233 to decrease the number of dimensions used to describe otolith shape variability while avoiding
234 collinearity between them and ensuring that the main sources of shape variation were kept
235 (Rohlf & Archie 1984). The selected principal components were gathered to construct the
236 otolith shape matrix \mathbf{S} with principal components of EFDs as columns and individuals as rows.
237 The otolith shape matrix \mathbf{S} was modelled using redundancy analysis (RDA) as depending on
238 three explanatory matrices: an individual matrix \mathbf{I} grouping individual-state variables and a
239 diet matrix \mathbf{D} derived from the diet composition:

$$240 \quad \mathbf{S} \sim \mathbf{I} + \mathbf{D} . \quad (2a)$$

241 The matrix \mathbf{I} was included in the model to disentangle and remove the effect of individual-
242 state as possible confounding factors on otolith shape. It was composed of fish age A as a factor
243 and total length L_T as a continuous effect to represent the ontogenetic effect on otolith shape,

244 sex S_e and maturity status M of the individual as factors potentially affecting fish physiology
245 and metabolism, and thus indirectly otolith biomineralization. The resulting model was:

$$246 \quad S \sim A + L_T + S_e + M + \mathbf{D} \quad (3a)$$

247 Alternatively, the potential confounding effect of environmental factors was also accounted for
248 by including an environmental matrix \mathbf{E} grouping external environmental factors in model 2:

$$249 \quad \mathbf{S} \sim \mathbf{I} + \mathbf{E} + \mathbf{D} . \quad (2b)$$

250 Matrix \mathbf{E} contained four variables to describe environmental conditions that may also affect
251 otolith biomineralization: temperature T and salinity S_a that were extracted from the
252 hydrodynamic model MARS 3D (Lazure & Dumas 2008) and averaged over the month of
253 October 2009, depth D_p that was measured at each sampling station during the survey, and
254 longitude and latitude ($L_o \times L_a$) of the sampling station. The resulting model was:

$$255 \quad \mathbf{S} \sim A + L_T + S_e + M + T + S_a + D_p + L_o \times L_a . \quad (3b)$$

256 The complete model described by Eq.3 (be it its version without 3a or with environmental
257 variables 3b) was reduced by stepwise selection based on significance (p-values) of the effects
258 determined by permutation tests (Borcard et al. 2011). Potential collinearity between
259 explanatory variables was checked by computing their Variance Inflation Factors (VIF) before
260 and after model reduction (Borcard et al. 2011). No strong collinearity (VIF<10) was detected
261 after mode reduction. Then, a variation partitioning was performed to estimate the percent
262 contribution of the two (\mathbf{I} and \mathbf{D}) or three (\mathbf{I} , \mathbf{E} and \mathbf{D}) reduced matrices to otolith shape
263 variation. The strict contribution of each reduced matrix to variation was tested using partial
264 redundancy analysis (pRDA) followed by a permutation tests, with the matrix for which the
265 contribution was estimated as an explanatory matrix and the other matrix or matrices depending

266 on model version (3a or 3b) as covariables. Standard deviation was computed for all fractions
267 of variation by bootstrapping. 500 bootstrap samples (random sampling with replacement) were
268 enough to obtain stable standard deviation estimates in all cases.

269 In order to answer the four main questions of the study, the previously described analysis was
270 performed with the diet matrix **D** constructed in four different ways (Fig. 3) as described below.

271 **Global relationship between diet and otolith shape (model 1, Fig. 3A)**

272 In order to estimate the potential global relationship between diet and otolith shape, matrix **D**
273 was composed of a number of selected correspondence axes resulting from a correspondence
274 analysis (CA) applied to the diet composition matrix based on taxonomic prey categories W_t .
275 Correspondence axes were selected according to the broken stick method. As for the PCA
276 applied to EDFs, this analysis was chosen to decrease the number of dimensions used to
277 describe fish diet variation and to remove collinearity between prey categories. Moreover, CA
278 is a method adapted to the analysis of species abundance data without pre-transformation
279 because abundance data within taxonomic prey categories are not normally distributed (Borcard
280 et al. 2011). Model reduction was performed while considering variables of matrix **I** (and **E**)
281 separately and matrix **D** as a whole. Hence, matrix **I** (and **E**) used in variation partitioning
282 was (were) reduced, while matrix **D** was not when kept in the reduced model.

283 **Prey categories involved in the relationship between diet and otolith shape (model 2, Fig.** 284 **3B)**

285 In this analysis, matrix **D** was simply set equal to the diet composition matrix based on
286 taxonomic prey categories W_t and model reduction was directly performed on Eq.3. Hence,
287 matrices **I** (, **E**) and **D** used in variation partitioning were all reduced. In order to identify the
288 main prey categories involved in diet-otolith shape co-variation, permutation tests were
289 performed for each selected prey category to test their significance. Moreover, to illustrate the

290 relationship between the prey categories selected and otolith shape, 8 predicted otolith outlines
291 were produced for each species in the following way.: A pRDA was performed on the otolith
292 shape matrix **S** with the selected prey categories as explanatory variables and the selected
293 individual-state (and environmental variables) as covariables. From this pRDA, 8 sets of
294 coordinates in the matrix **S** space were predicted at the 8 combinations of ± 1 standard deviation
295 (sd) along the two first axes of the pRDA $\{(+sd_1,0),(-sd_1,0),(+sd_1,+sd_2),(-sd_1,+sd_2),$
296 $(+sd_1,-sd_2),(-sd_1,-sd_2),(0,+sd_2),(0,-sd_2)\}$ representing variation in linear combinations
297 of the selected prey categories. Predictions in the matrix **S** space were then projected back to
298 the matrix **F** space to produce predicted *EFDs* that were then used to draw predicted otolith
299 shapes on the pRDA biplot.

300 **Contribution of diet relative composition vs food quantity to diet-otolith shape co-** 301 **variation (model 3, Fig. 3C)**

302 In this analysis, matrix **D** was decomposed into a matrix representing the relative diet
303 composition based on taxonomic prey categories **C** and a vector representing food quantity **Q**
304 . The relative diet composition matrix **C** was obtained by performing a CA on the matrix of
305 relative contribution of taxonomic prey categories to diet composition $\%W_{t,j}$ and selecting
306 correspondence axes according to the broken stick method. The vector **Q** gathered the total
307 weight of the stomach content of each individual, in other words the sums along rows $\sum_j w_{t,ij}$
308 of the diet composition matrix **W_t**. In order to ensure that matrices **C** and **Q** were kept in the
309 reduced model (with the ultimate aim to estimate their relative contribution to otolith shape
310 variation), model reduction was based on a pRDA where the otolith shape matrix **S** was
311 explained by matrix **I** (and **E**) while matrices **C** and **Q** were considered as covariables.
312 Hence, matrix **I** (and **E**) used in variation partitioning were reduced, while matrices **C** and
313 **Q** were not.

314 **Relationship between diet energy composition and otolith shape (model 4, Fig. 3D)**

315 In this last analysis, matrix **D** was set equal to the diet composition matrix based on energetic
316 prey categories W_e . Model reduction and variation partitioning were then performed as for
317 model 1.

318 All statistical analyses were performed using the package *vegan* (Oksanen et al. 2013) in the
319 statistical environment R.3.1.1 (R Core Team 2014). The R codes used in this study are
320 available from the authors upon request.

321

322

323 **Results**

324 Only results based on models without environmental confounding factors (Eq. 3a) are presented
325 in details in this section. The rationale is that considering environmental variables at sampling
326 site as related to otolith shape implies assuming that these environmental conditions are
327 representative of those experienced by individuals during a substantial part of their life, which
328 is subject to controversy for mobile organisms such as fish (see Discussion section). Only
329 important differences between the results without and with environmental factors will be
330 highlighted here. Detailed results when accounting for environmental factors (Eq.3b) can be
331 found in Tables S2-S4-S5 and Figures S1-S2 in Supplementary material. In addition, the effects
332 of individual-state variables on otolith shape have already been studied in detail (Hüssy 2008,
333 Capoccioni et al. 2011). They were accounted for in the analyses to avoid potential confounding
334 effects but were not the main focus of this study. Consequently, their effects are not detailed
335 here but can be found in Tables S3-S4 in Supplementary material.

336

337 **Global relationship between diet and otolith shape (model 1)**

338 The reduced models explained between 11% and 26% of otolith shape variability for roundfish
339 species. For flatfish species, percentages of explained variation were higher: 14% and 38% for
340 plaice and sole, respectively (Table 2). Variation partitioning revealed that the individual matrix
341 **I** explained the greatest part of variation in otolith shape for all species, between 19% and 27%,
342 except for red gurnard and European plaice for which it was not significant (Fig.4, first column).
343 For all species, a significant diet contribution was detected at an alpha threshold of 5%, except
344 for tub gurnard and European plaice for which it was significant at an alpha threshold of 10%
345 only. Matrix **D** explained between 10% and 16% of otolith shape variability (Fig.4). When
346 including the environmental matrix **E** in the analysis, a significant diet contribution was
347 detected at an alpha threshold of 5% for European plaice that accounted for 13% of variation
348 (Fig.S1, first column; Table S2).

349

350 **Prey categories involved in the relationship between diet and otolith shape (model 2)**

351 Between 2 to 7 taxonomic prey categories were selected in the reduced model according to
352 species (Table 2) except for tub gurnard for which no taxonomic prey category was selected
353 and hence no reduced model was tested. Explained variation by model 2 varied between 25%
354 and 35% according to species. As in model 1, the individual matrix **I** had a significant effect
355 on otolith shape for all species (Fig.4, second column). It explained between 14% and 23% of
356 shape variability. Concerning taxonomic prey categories, a significant contribution to otolith
357 shape variation was detected for all species except one, tub gurnard (see above). The selected
358 categories explained between 11% and 201% of otolith shape variability, which was slightly
359 higher than the global effect of diet in model 1. According to species, the taxonomic prey
360 categories contributing significantly differed in terms of relative frequency of occurrence $\%F_j$
361 and relative contribution of prey categories to diet $\%W_j$. For striped red mullet, the significant
362 taxonomic prey categories (Fig. 5) were either primary ones, i.e., characterized by a high $\%F_{t,j}$

363 and high $\%W_{t,j}$ such as *annelida*, or intermediary ones, i.e., characterized by a small $\%W_j$
364 with respect to $\%F_j$ such as *caridea*, or secondary ones, i.e., with a low $\%F_j$ and small $\%W_j$
365 such as *bivalvia*, *brachyoura*, and *decapoda* larvae (Fig.2). Similarly for red gurnard, influential
366 taxonomic prey categories were either primary ones such as *caridea* or secondary ones such as
367 *gastropoda*. For European plaice, only a primary taxonomic prey category was related to otolith
368 shape, namely *Echinodermata*, contrary to common sole, for which only a secondary
369 taxonomic prey category, *cnidaria*, was linked to otolith shape. When including the
370 environmental matrix **E** in the analysis, the contribution of taxonomic prey categories to otolith
371 shape variation increased to 40% for red gurnard but was relatively stable for the other species
372 (Fig.S1, second column; Table S2).

373 Predicted otolith shapes as reconstructed in Fig. 5 revealed that diet was related to global otolith
374 shape through the length/width ratio and thus otoliths' ellipticity, but also to finer details.
375 Variations occurred in the otolith crenations, the width of the *excisura major* (the indentation
376 between the rostrum and the antirostrum (Panfili et al. 2002), the length of the rostrum and the
377 antirostrum, and the posterior part of the otolith shape.

378

379 **Contribution of relative diet composition vs food quantity to diet-otolith shape co-** 380 **variation (model 3)**

381 For tub gurnard, model 3 was not estimated given the absence of diet effect in model 1 (and
382 subsequently model 2). For the other species, model 3 explained between 9% and 37% of otolith
383 shape variability (Table 2). Variation partitioning gave similar results in terms of individual
384 effects to those obtained with model 1 except for European plaice for which the explained
385 variation by the individual matrix **I** increased strongly (Fig.4, first and third columns, fourth
386 line). Regarding diet, relative composition **C** contributed significantly to otolith shape variation
387 for striped red mullet, red gurnard and common sole. Its effect explained 12% to 16% of

388 variation. No significant contribution of **C** was found for European plaice even if variation
389 partitioning attributed 8% of otolith shape variation to this matrix. In contrast, when the
390 environmental matrix **E** was added in the model, a significant contribution of **C** was detected
391 for European plaice while significance disappeared for common sole despite the slight decrease
392 in percentage of variation explained (Fig.S1, third column; Table S2). Contrary to diet relative
393 composition **C**, food quantity **Q** did not contribute significantly to otolith shape variation
394 whatever the species, including and excluding the environmental matrix **E** in the modele.

395

396 **Relationship between diet energy composition and otolith shape (model 4)**

397 The reduced models explained between 5% and 28% of otolith shape variation (Table 2).
398 Variation partitioning revealed that the individual matrix **I** explained the greatest part of
399 variation in otolith shape for all species, between 5% and 27 (Fig.4, fourth column). A
400 significant contribution of diet energetic composition was detected for tub gurnard and
401 European plaice only and at an alpha threshold of 5% and 10%, respectively. Matrix **D**
402 explained 12% and 8% of otolith shape variation, respectively (Fig.4, fourth column).

403

404 **Discussion**

405 In this study, we found that individual-state variables contributed the largest fraction of otolith
406 shape variation in most cases. This result was expected given the already well described effect
407 of individual-state variables on otolith shape and we will not discuss it here as there is ample
408 literature on the subject (Cardinale et al. 2004, Hüsey 2008, Capoccioni et al. 2011). Besides
409 this known effect, we showed an intra-population relationship between diet and otolith shape
410 for all fish species studied, although the relationship was less robust for tub gurnard. For the
411 latter, only the relationship between diet energetic composition and otolith shape was
412 significant at an alpha threshold of 5%, the global relationship between diet weight composition

413 and otolith shape being significant at an alpha threshold of 10% only. Small sample size of this
414 species compared to the others may explain a lower power of signal detection. Then we were
415 able to relate either primary, intermediary or secondary prey categories to otolith shape
416 variations. Moreover, otolith reconstructions suggest that these variations could affect both
417 global shape and its finer details. Then, by comparing the contributions of food composition
418 and quantity, we showed that food composition contributed more largely to otolith shape
419 variation than the quantity of food ingested by fish. Finally, for only two species, a diet
420 influence based on energetic content categories was detected significant.

421

422 **The role of organic matrix composition in otolith biomineralization**

423 Although the organic matrix of sagittal otoliths represents a minor fraction of the total material
424 (Carlström 1963, Degens et al. 1969), it plays an important role in otolith formation. It actually
425 controls the nucleation, the crystallization, the orientation and the morphology as well as the
426 polymorphism of crystal units the otolith is composed of (Nagasawa 2013). The organic matrix
427 is mainly composed of proteins, amino acids (AAs), collagens and proteoglycans, which
428 precursors are secreted by the saccular epithelium in the endolymph (Payan et al. 2004).
429 However, only 3 major proteins are present in their definite form both in the endolymph and
430 the otolith. This suggests that the organic matrix is not directly composed of compounds present
431 in endolymph but also of proteins derived from the modification of precursors during their
432 deposition onto the otolith (Borelli et al. 2001). McMahon et al. (2010) observed that AAs'
433 $\delta^{13}\text{C}$ values in fish muscle and in their diet co-varied, with significant differences diet
434 treatments. Moreover, they showed that AAs' $\delta^{13}\text{C}$ values in muscles and in otoliths were
435 correlated with a slope around 1 and thus recorded an identical dietary information (McMahon
436 et al. 2011). Consequently, the AAs found in otolith proteins come from the food consumed by
437 fish.

438 Otolith shape is determined by its crystalline architecture (calcium carbonate CaCO₃). Several
439 proteins are known to control the CaCO₃ polymorphism (aragonite, calcite or vaterite) and the
440 morphology of its crystal units. Starmaker (Söllner et al. 2003) and Otolith Matrix
441 Macromolecule-64 (OMM-64) (Tohse et al. 2009) are water-soluble and acidic (due to a
442 calcium-binding region rich in glutamate) glycoproteins involved in the control of crystal
443 polymorphism (Nagasawa 2013). The Otolith Matrix Protein-1 (OMP-1) is another water-
444 soluble protein required for normal otolith growth and for the deposition of another otolith
445 protein, otolin-1. The latter is a collagenous protein that makes up the structural network for
446 subsequent calcification, and thus stabilizes the otolith's mineral and organic fractions and
447 insures the correct arrangement of otoliths on the sensory epithelium (Murayama et al. 2005).

448

449 **Potential mechanisms underlying the relationship between diet composition and otolith** 450 **shape**

451 In the present study, a significant relationship between diet taxonomic composition and otolith
452 shape was detected for all species except for one. According to the taxonomic prey categories
453 consumed, otolith shape presented some variations in both global shape, such as the degree of
454 ellipticity, and finer details, such as otolith crenation or the width of the *excisura major*. Two
455 hypotheses, or a combination of both, could explain the correlation between otolith shape and
456 diet taxonomic composition. First, the total quantity of proteins in the saccular endolymph could
457 vary according to the quantity of proteins in the prey consumed, which would affect the rate of
458 organic matrix synthesis and thus CaCO₃ deposition and ultimately otolith growth. Protein
459 consumption has been known to have the highest regulatory impact on protein synthesis
460 (Houlihan et al. 1988). Consequently, diet taxonomic composition could influence “global”
461 otolith shape through effects on otolith growth. Secondly, the proteic composition of the organic
462 matrix, i.e. the relative quantity of water-soluble, water-insoluble and insoluble proteins, may

463 change according to food composition, which would impact the crystal structure (orientation,
464 morphology, and polymorphism) of precipitated CaCO_3 and, thus, otolith shape. More
465 precisely, food composition varies in terms of proteins or even AAs, whether essential (e.g.
466 leucine) or not (e.g. glutamic acid), that are necessary for the synthesis of some otolith matrix
467 proteins involved in the control of crystal structure (Asano & Mugiya 1993, Davis et al. 1995,
468 Sasagawa & Mugiya 1996, Nagasawa 2013). Consequently, food proteic composition could
469 have a direct contribution to variations in otolith crenation or/and an indirect contribution
470 through its effect on otolith growth, which impacts global otolith shape. In addition, some
471 proteoglycan and polysaccharide are present in both the saccular endolymph and the organic
472 matrix (Murayama et al. 2005). Even if their role in otolith biomineralization is unknown,
473 variability in their quantity and composition in prey could also impact otolith shape in the same
474 way as proteins.

475 Diet energetic composition was significantly related to otolith shape in two species only.
476 Contrary to proteins and glucids, lipids are not components of the otolith organic matrix, which
477 could explain the absence of a strong relationship between the diet energetic composition and
478 otolith shape. Lipids are indeed the main determinant of prey energetic content as energy per
479 unit of mass in prey is positively correlated to their lipid content and generally negatively
480 correlated to their protein content (Spitz et al. 2010). The fact that diet taxonomic composition
481 was better correlated with otolith shape variation than diet energetic composition suggests that
482 prey lipid versus protein content is less related to otolith shape variation than prey composition
483 (in opposition to amount) in terms of proteins and carbonates. This result seems rather logical
484 given the composition of the otolith and its precursors when thinking about a direct effect on
485 otolith shape through its organic matrix. In contrast, it may seem surprising when envisaging
486 an indirect effect on otolith shape through otolith growth. High dietary lipid levels can improve
487 body size growth (Vergara et al. 1999, Boujard et al. 2004). Diet lipid content is thus likely to

488 be related to otolith growth and thus shape. The lack of strong relationship could result from
489 several aspects. First, high dietary protein levels also favour faster growth. Given that lipid and
490 protein levels in diet are oppositely correlated to diet energy content (Spitz et al. 2010), the two
491 effects could cancel each other out when considering the effect of diet energetic composition.
492 Second, some of the reduced models included a size effect that could absorb the indirect effect
493 of diet energetic composition through growth. Third, diet energetic composition was based on
494 3 qualitative, relatively coarse, energetic prey categories, which may not be precise enough to
495 detect a relationship. Studies based on a proper quantification of diet energy content, through
496 bomb calorimetry of stomach contents for instance, or on the lipid composition of prey would
497 allow to investigate further the potential relationship between diet energy content and otolith
498 shape.

499 In this study, locations of variation in otolith shape related to food composition were identified
500 from reconstructed shapes. Although these reconstructions were “caricatures” predicted from a
501 statistical model limited to individuals from the eastern English Channel and to our observations
502 in terms of individual-state, they highlighted the large number of otolith shape areas co-varying
503 with food composition suggesting the importance of understanding otolith biomineralization
504 3D processes. Otolith shape variation could be also explained by variations of spatial
505 distribution of precursors due to some physical constraints on the saccule which would impact
506 the otolith shape. However, the current lack of knowledge regarding such processes prevents
507 from clearly evaluating the likelihood of this hypothesis.

508

509 **Absence of relationship between food quantity and otolith shape**

510 No significant relationship between food quantity and otolith shape was detected in this study.
511 This result contrasts with several works that showed experimentally that food quantity impacted
512 otolith shape both indirectly via variation in otolith growth creating variation in “global” otolith

513 shape and directly on otolith crenations (Gagliano & McCormick 2004, Cardinale et al. 2004,
514 Hüsey 2008). We could raise the assumption that in the present study, the quantity of ingested
515 food did not differ sufficiently between individuals in order to observe a significant influence
516 on otolith shape. Likewise, Hüsey (2004) did not observed any effect of food quantity on otolith
517 opacity and on the ratio between water-soluble and water- insoluble proteins in the organic
518 matrix whereas, under more severe food restriction for a longer period, Høie et al (2008)
519 observed that more translucent otolith material was deposited. Such apparent discrepancies are
520 well reconciled under the light of temperature and food effect interactions (either synergetic or
521 antagonistic) on otolith opacity (Fablet et al. 2011). Moreover, here food quantity was measured
522 as the sum of the weights of all prey items found in an individual's stomach. However, prey
523 items in stomach contents are digested at varying degrees according to individuals, which can
524 introduce a bias in the estimation of inter-individual differences in ingested food quantity
525 (Gannon 1976).

526

527 **Limitations of the study**

528 The imprecision of food quantity measure highlights a potential, more general, limitation of
529 stomach content analysis that only provides a snapshot of fishes' diet, and in this precise case
530 at a single season as all fish in this study have been sampled in October. The interpretation of
531 the results in the present study rely on the assumption that observed inter-individual differences
532 in diet are consistent over a sufficiently long time period to be related to inter-individual otolith
533 shape differences. It should be noted here that the assumption is concerned with the
534 representativity of inter-individual differences, i.e. individuals' specialization, and not of
535 individuals' diet itself. In other words, the assumption is that diet difference at a given time
536 gives an index of dietary specialization even though individuals' diet may vary through time.
537 To our knowledge, such an assumption has never been directly confirmed nor invalidated in

538 fish given that no longitudinal study on fish diet, i.e. with repeated observations of prey
539 selectivity or stomach content on the same individuals, was performed for testing. Although the
540 possibility that this hypothesis does not hold cannot be totally ruled out, several arguments can
541 be brought in its support. There is ample literature on the importance and prevalence of
542 individual diet specialization (see reviews in Bolnick et al. 2003; Araújo et al. 2011), notably
543 long-term trophic specialization in freshwater and marine vertebrates (e.g. Bearhop et al. 2006,
544 Newsome et al. 2009, Hückstädt et al. 2011, Rosenblatt et al. 2015) including fish (e.g.
545 Beaudoin et al. 1999, Svanbäck & Persson 2004, Matich et al. 2011), that support this
546 assumption based on isotopic data. Consistent inter-individual differences in several
547 behavioural traits that may affect diet have also been documented in fish (see review in
548 Mittelbach et al. 2014) such as habitat use and movements (e.g. Matich & Heithaus 2015) or
549 boldness (e.g. Ward et al. 2004, Harcourt et al. 2009). A more technical argument is that the
550 presence of multiple prey items per stomach ensures that cross-sectional samples of individuals'
551 diet are relevant to estimate individual diet specialization (Araújo et al. 2011). An additional
552 argument in support of our assumption comes from the relative stability of our results across
553 the three different analyses based on taxonomic prey categories for each species and the relative
554 low standard deviations of fractions in variation partitioning obtained from bootstrapping
555 analyses (Table 3, Table.S5). It should also be noted that, despite its limitations, stomach
556 content analysis is the only way to obtain an indication of ingested food quantity in natural
557 condition. In contrast, carbon stable isotope ratios could provide a temporally-integrated view
558 of individuals' diet composition and account for seasonal changes in diet, but without allowing
559 the quantification of the amount of food ingested. Additionally, the precise identification of the
560 consumed prey items from carbon stable isotope ratios by using so-called mixing models
561 requires knowledge of the isotopic ratios of all potential preys and of the isotopic fractionation
562 between preys and consumers (Post 2002, Fry 2007). Still, variation of carbon stable isotope

563 ratio (in muscles and/or otolith) across individuals could be used to describe variability in
564 individual diet composition with the aim of linking it to the otolith shape variability. This would
565 complement the results obtained in this study.

566 Likewise, the environmental variables considered in our supplementary analyses (see
567 Supplementary material Fig.S1-S2 and Tables S2-S4), i.e. temperature, depth, salinity,
568 longitude and latitude, were a snapshot of the environment experienced by individuals as they
569 were measured at sampling site and averaged over a single month. Similarly to stomach
570 contents, their use in the analyses (Eq. 2b and 3b) relies on the assumption that they are
571 representative of inter-individual differences in the environment experienced over a sufficiently
572 long-time period to be related to otolith shape. Such an assumption may seem unlikely for a
573 majority of fish given their mobility, which could explain the fact that for a majority of the
574 studied species, the environmental matrix was not significantly related to otolith shape (Fig.S1).
575 However, for European plaice, the inclusion of the environmental matrix in the analysis has
576 allowed describing a supplementary part of otolith shape variation that, it seems, was obscuring
577 the diet signal since the diet matrix also became significant. This result may be linked to the
578 supposedly lower mobility of benthic flatfish such as plaice. In order to have a temporally-
579 integrated view of the environment experienced by individuals possibly accounting also for
580 seasonality, otolith chemistry such as the variation of oxygen isotopic ratios as an index for
581 temperature (Kalish 1991) or the ratio Sr/Ca as an index for the salinity (Secor 1992) could be
582 used in future studies. Moreover, all fish in this study have been sampled in October, i.e. in a
583 single season. It would be interesting to consider the implication of seasonality on the
584 relationship between diet and environment on the one hand and otolith shape on the other.

585

586 In summary, an intra-population relationship between diet and otolith shape was detected for
587 several roundfish and flatfish species from the eastern English Channel. Detailed analyses

588 revealed that both main and secondary prey categories were involved in this relationship and
589 that variations influenced both the otolith's global shape and some finer details. The
590 contribution of relative diet taxonomic composition to otolith shape variation was much higher
591 than that of ingested food quantity represented by the weight of prey items. Finally, diet
592 energetic composition was correlated with otolith shape of only one species and marginally for
593 another. Gagliano and McCormick (2004) had suggested that otolith shape could be used to
594 discriminate fine scale events, such as the magnitude and periodicity of feeding in wild fish
595 populations, in addition to the discrimination of stocks and populations based on coarser aspects
596 such as life-history differences. The present study shows that diet composition may also be a
597 source of otolith shape variability within populations through direct and/or indirect (via otolith
598 growth) processes. This introduces a novel potential interpretation of three classically known
599 effects on otolith shape. First, otolith shape variation across age and size is generally assigned
600 to ontogenetic changes in metabolism and physiology (Campana & Casselman 1993, Mérigot
601 et al. 2007). Ontogenetic changes in diet composition could also contribute directly to otolith
602 shape variation, thereby acting as a confounding factor (Morat et al. 2012, Vignon 2012).
603 Likewise, sexual dimorphism in otolith shape is generally attributed to physiological
604 differences between sexes. However, sexual dimorphism in diet composition, especially at the
605 time of mating, has been documented in several fish species (Casselman & Schulte-Hostedde
606 2004, Tsuboi et al. 2011) and could thus also explain otolith shape dimorphism. Finally,
607 environmental abiotic factors, such as temperature and salinity, are also known to influence
608 otolith shape variation (Lombarte & Leonart 1993) and spatial variation in otolith shape are
609 often interpreted as resulting from habitat differentiation (Morat et al. 2012). However, such
610 variation in abiotic factors is generally related to differences in prey categories available to
611 individual predator, such that geographical variations in diet composition could also generate
612 geographical variation in otolith shape (Vignon 2012). Such applied consequences call for

613 further investigations of the sources of otolith shape variation and their mechanistic effect on
614 biomineralization, notably those related to diet.

615

616 **References**

617 Allemand D, Mayer-Gostan N, De Pontual H, Boeuf G, Payan P (2007) Fish Otolith Calcification in
618 Relation to Endolymph Chemistry. In: Bäuerlein E (ed) Handbook of Biomineralization. Wiley-
619 VCH Verlag GmbH, p 291–308

620 Amara R, Meziane T, Gilliers C, Hermel G, Laffargue P (2007) Growth and condition indices in juvenile
621 sole *Solea solea* measured to assess the quality of essential fish habitat. *Mar Ecol Prog Ser*
622 351:201–208

623 Anthony JA, Roby DD, Turco KR (2000) Lipid content and energy density of forage fishes from the
624 northern Gulf of Alaska. *J Exp Mar Biol Ecol* 248:53–78

625 Araújo MS, Bolnick DI, Layman CA (2011) The ecological causes of individual specialisation. *Ecol Lett*
626 14:948–958

627 Asano M, Mugiya Y (1993) Biochemical and calcium-binding properties of water-soluble proteins
628 isolated from otoliths of the tilapia, *Oreochromis niloticus*. *Comp Biochem Physiol Part B*
629 *Comp Biochem* 104:201–205

630 Bearhop S, Phillips RA, McGill R, Cherel Y, Dawson DA, Croxall JP (2006) Stable isotopes indicate sex-
631 specific and long-term individual foraging specialisation in diving seabirds. *Mar Ecol Prog Ser*
632 311:157–164

633 Beaudoin CP, Tonn WM, Prepas EE, Wassenaar LI (1999) Individual specialization and trophic
634 adaptability of northern pike (*Esox lucius*): an isotope and dietary analysis. *Oecologia*
635 120:386–396

636 Bolles KL, Begg GA (2000) Distinction between silver hake (*Merluccius bilinearis*) stocks in US waters
637 of the northwest Atlantic based on whole otolith morphometrics. *Fish Bull* 98:451–462

638 Bolnick DI, Svanbäck R, Fordyce JA, Yang LH, Davis JM, Hulseley CD, Forister ML (2003) The Ecology of
639 Individuals: Incidence and Implications of Individual Specialization. *Am Nat* 161:1–28

640 Borcard D, Gillet F, Legendre P (2011) *Numerical Ecology with R*. Springer

641 Borelli G, Mayer-Gostan N, Pontual H de, Boeuf G, Payan P (2001) Biochemical Relationships
642 Between Endolymph and Otolith Matrix in the Trout (*Oncorhynchus mykiss*) and Turbot
643 (*Psetta maxima*). *Calcif Tissue Int* 69:356–364

644 Boujard T, Gélineau A, Covès D, Corraze G, Dutto G, Gasset E, Kaushik S (2004) Regulation of feed
645 intake, growth, nutrient and energy utilisation in European sea bass (*Dicentrarchus labrax*)
646 fed high fat diets. *Aquaculture* 231:529–545

647 Buckel JA, Sharack BL, Zdanowicz VS (2004) Effect of diet on otolith composition in *Pomatomus*
648 *saltatrix*, an estuarine piscivore. *J Fish Biol* 64:1469–1484

- 649 Caldwell C, Wellington GM (2003) Patterns of annual increment formation in otoliths of pomacentrids
650 in the tropical western Atlantic: implications for population age-structure examination. *Mar*
651 *Ecol Prog Ser* 265:185–195
- 652 Campana SE, Casselman JM (1993) Stock Discrimination Using Otolith Shape Analysis. *Can J Fish*
653 *Aquat Sci* 50:1062–1083
- 654 Capoccioni F, Costa C, Aguzzi J, Menesatti P, Lombarte A, Ciccotti E (2011) Ontogenetic and
655 environmental effects on otolith shape variability in three Mediterranean European eel
656 (*Anguilla anguilla*, L.) local stocks. *J Exp Mar Biol Ecol* 397:1–7
- 657 Cardinale M, Doering-Arjes P, Kastowsky M, Mosegaard H (2004) Effects of sex, stock, and
658 environment on the shape of known-age Atlantic cod (*Gadus morhua*) otoliths. *Can J Fish*
659 *Aquat Sci* 61:158–167
- 660 Carlström D (1963) A Crystallographic Study of Vertebrate Otoliths. *Biol Bull* 125:441–463
- 661 Casselman SJ, Schulte-Hostedde AI (2004) Reproductive roles predict sexual dimorphism in internal
662 and external morphology of lake whitefish, *Coregonus clupeaformis*. *Ecol Freshw Fish*
663 13:217–222
- 664 Castonguay M, Simard P, Gagnon P (1991) Usefulness of Fourier Analysis of Otolith Shape for Atlantic
665 Mackerel (*Scomber scombrus*) Stock Discrimination. *Can J Fish Aquat Sci* 48:296–302
- 666 Coppin F, Carpentier A, Delpech J-P, Schlaich I (2002) Manuel des protocoles de campagne
667 halieutique. Campagnes CGFS. V 3.
- 668 Dauvin J-C, Joncourt M (1989) Energy Values of Marine Benthic Invertebrates from the Western
669 English Channel. *J Mar Biol Assoc U K* 69:589–595
- 670 Davis JG, Oberholtzer JC, Burns FR, Greene MI (1995) Molecular cloning and characterization of an
671 inner ear-specific structural protein. *Science* 267:1031–1034
- 672 Degens ET, Deuser WG, Haedrich RL (1969) Molecular structure and composition of fish otoliths. *Mar*
673 *Biol* 2:105–113
- 674 Elsdon TS, Ayvazian S, McMahon KW, Thorrold SR (2010) Experimental evaluation of stable isotope
675 fractionation in fish muscle and otoliths. *Mar Ecol Prog Ser* 408:195–205
- 676 Fablet R, Pecquerie L, Pontual H de, Høie H, Millner R, Mosegaard H, Kooijman SALM (2011) Shedding
677 Light on Fish Otolith Biomineralization Using a Bioenergetic Approach. *PLoS ONE* 6:e27055
- 678 Fernandez-Jover D, Sanchez-Jerez P (2015) Comparison of diet and otolith growth of juvenile wild fish
679 communities at fish farms and natural habitats. *ICES J Mar Sci J Cons* 72:916–929
- 680 Fraser AJ (1989) Triacylglycerol Content as a Condition Index for Fish, Bivalve, and Crustacean Larvae.
681 *Can J Fish Aquat Sci* 46:1868–1873
- 682 Fry B (2007) *Stable Isotope Ecology*. Springer Science & Business Media
- 683 Gagliano M, McCormick M (2004) Feeding history influences otolith shape in tropical fish. *Mar Ecol*
684 *Prog Ser* 278:291–296

- 685 Gannon JE (1976) The Effects of Differential Digestion Rates of Zooplankton by Alewife, *Alosa*
686 *pseudoharengus*, on Determinations of Selective Feeding. *Trans Am Fish Soc* 105:89–95
- 687 Godfriaux BL (1969) Food of predatory demersal fish in Hauraki Gulf. *N Z J Mar Freshw Res* 3:518–544
- 688 Guibbolini M, Borelli G, Mayer-Gostan N, Priouzeau F, De Pontual H, Allemand D, Payan P (2006)
689 Characterization and variations of organic parameters in teleost fish endolymph during day–
690 night cycle, starvation and stress conditions. *Comp Biochem Physiol A Mol Integr Physiol*
691 145:99–107
- 692 Harcourt JL, Ang TZ, Sweetman G, Johnstone RA, Manica A (2009) Social Feedback and the
693 Emergence of Leaders and Followers. *Curr Biol* 19:248–252
- 694 Høie H, Folkvord A, Mosegaard H, Li L, Clausen LAW, Norberg B, Geffen AJ (2008) Restricted fish
695 feeding reduces cod otolith opacity. *J Appl Ichthyol* 24:138–143
- 696 Houlihan DF, Hall SJ, Gray C, Noble BS (1988) Growth Rates and Protein Turnover in Atlantic Cod,
697 *Gadus morhua*. *Can J Fish Aquat Sci* 45:951–964
- 698 Hückstädt LA, Koch PL, McDonald BI, Goebel ME, Crocker DE, Costa DP (2011) Stable isotope analyses
699 reveal individual variability in the trophic ecology of a top marine predator, the southern
700 elephant seal. *Oecologia* 169:395–406
- 701 Hüsey K (2008) Otolith shape in juvenile cod (*Gadus morhua*): Ontogenetic and environmental
702 effects. *J Exp Mar Biol Ecol* 364:35–41
- 703 Hüsey K, Mosegaard H (2004) Atlantic cod (*Gadus morhua*) growth and otolith accretion
704 characteristics modelled in a bioenergetics context. *Can J Fish Aquat Sci* 61:1021–1031
- 705 Hüsey K, Mosegaard H, Jessen F (2004) Effect of age and temperature on amino acid composition and
706 the content of different protein types of juvenile Atlantic cod (*Gadus morhua*) otoliths. *Can J*
707 *Fish Aquat Sci* 61:1012–1020
- 708 Huuskonen H, Karjalainen J (1998) A preliminary study on the relationships between otolith
709 increment width, metabolic rate and growth in juvenile whitefish (*Coregonus lavaretus* L.).
710 *Arch Für Hydrobiol* 142:371–383
- 711 ICES (2010) Report of the Workshop on Age Reading of North Sea (IV) and Skagerrak-Katt egat (IIIa)
712 Plaice (WKARP), 2- 5 November 2010 , Ijmuiden, The Netherlands . ICES CM 2010/ACOM: 45 .
713 65 pp.
- 714 ICES (2012) Report of the workshop on age reading of red mullet and striped red mullet, 2–6 July
715 2012, Boulogne-sur-Mer, France. ICES CM2012/ACOM:60.52pp.
- 716 ICES (2014) Report of the Workshop for maturity staging chairs (WKMATCH), 11–15 June 2012, Split,
717 Croatia. ICES CM 2012/ACOM:58. 57 pp.
- 718 Jolivet A, Bardeau J-F, Fablet R, Paulet Y-M, Pontual H de (2013) How do the organic and mineral
719 fractions drive the opacity of fish otoliths? Insights using Raman microspectrometry. *Can J*
720 *Fish Aquat Sci* 70:711–719
- 721 Kalish JM (1991) Oxygen and carbon stable isotopes in the otoliths of wild and laboratory-reared
722 Australian salmon (*Arripis trutta*). *Mar Biol* 110:37–47

- 723 Kuhl FP, Giardina CR (1982) Elliptic Fourier features of a closed contour. *Comput Graph Image*
724 *Process* 18:236–258
- 725 L'Abée-Lund JH (1988) Otolith shape discriminates between juvenile Atlantic salmon, *Salmo salar* L.,
726 and brown trout, *Salmo trutta* L. *J Fish Biol* 33:899–903
- 727 Lazure P, Dumas F (2008) An external–internal mode coupling for a 3D hydrodynamical model for
728 applications at regional scale (MARS). *Adv Water Resour* 31:233–250
- 729 Lestrel PE (2008) *Fourier Descriptors and Their Applications in Biology*. Cambridge University Press
- 730 Lombarte A, Leonart J (1993) Otolith size changes related with body growth, habitat depth and
731 temperature. *Environ Biol Fishes* 37:297–306
- 732 Mahé K, Moerman M, Holmes I, Boiron A, Elleboode R (2012) Report of the Sole (*Solea solea*) in the
733 Bay of Biscay Otolith Exchange Scheme 2011. :14 pp
- 734 Massou AM, Panfili J, Laë R, Baroiller JF, Mikolasek O, Fontenelle G, Le Bail P-Y (2002) Effects of
735 different food restrictions on somatic and otolith growth in Nile tilapia reared under
736 controlled conditions. *J Fish Biol* 60:1093–1104
- 737 Matich P, Heithaus MR (2015) Individual variation in ontogenetic niche shifts in habitat use and
738 movement patterns of a large estuarine predator (*Carcharhinus leucas*). *Oecologia* 178:347–
739 359
- 740 Matich P, Heithaus MR, Layman CA (2011) Contrasting patterns of individual specialization and
741 trophic coupling in two marine apex predators. *J Anim Ecol* 80:294–305
- 742 McMahon KW, Fogel ML, Elsdon TS, Thorrold SR (2010) Carbon isotope fractionation of amino acids
743 in fish muscle reflects biosynthesis and isotopic routing from dietary protein. *J Anim Ecol*
744 79:1132–1141
- 745 Mérigot B, Letourneur Y, Lecomte-Finiger R (2007) Characterization of local populations of the
746 common sole *Solea solea* (Pisces, Soleidae) in the NW Mediterranean through otolith
747 morphometrics and shape analysis. *Mar Biol* 151:997–1008
- 748 Mittelbach GG, Ballew NG, Kjelvik MK (2014) Fish behavioral types and their ecological
749 consequences. *Can J Fish Aquat Sci* 71:927–944
- 750 Molony BW, Choat JH (1990) Otolith increment widths and somatic growth rate: the presence of a
751 time-lag. *J Fish Biol* 37:541–551
- 752 Molony BW, Sheaves MJ (1998) Otolith increment widths and lipid contents during starvation and
753 recovery feeding in adult *Ambassis vachelli* (Richardson). *J Exp Mar Biol Ecol* 221:257–276
- 754 Morat F, Letourneur Y, Nérini D, Banaru D, Batjakas LE (2012) Discrimination of red mullet
755 populations (Teleostean, Mullidae) along multi-spatial and ontogenetic scales within the
756 Mediterranean basin on the basis of otolith shape analysis. *Aquat Living Resour* 25:27–39
- 757 Mosegaard H, Svedäng H, Taberman K (1988) Uncoupling of Somatic and Otolith Growth Rates in
758 Arctic Char (*Salvelinus alpinus*) as an Effect of Differences in Temperature Response. *Can J*
759 *Fish Aquat Sci* 45:1514–1524

760 Murayama E, Herbomel P, Kawakami A, Takeda H, Nagasawa H (2005) Otolith matrix proteins OMP-1
761 and Otolin-1 are necessary for normal otolith growth and their correct anchoring onto the
762 sensory maculae. *Mech Dev* 122:791–803

763 Nagasawa H (2013) The Molecular Mechanism of Calcification in Aquatic Organisms. *Biosci*
764 *Biotechnol Biochem* 77:1991–1996

765 Newsome SD, Tinker MT, Monson DH, Oftedal OT, Ralls K, Staedler MM, Fogel ML, Estes JA (2009)
766 Using stable isotopes to investigate individual diet specialization in California sea otters
767 (*Enhydra lutris nereis*). *Ecology* 90:961–974

768 Norrbin F, Båmstedt U (1984) Energy contents in benthic and planktonic invertebrates of
769 Kosterfjorden, Sweden. A comparison of energetic strategies in marine organism groups.
770 *Ophelia* 23:47–64

771 Oksanen J, Blanchet FG, Kindt R, Legendre P, Minchin PR, O’Hara RB, Simpson GL, Peter S, Stevens
772 MHH, Wagner H (2013) *vegan: Community Ecology* Package. R package version 2.0-10.

773 Panfili J, De Pontual H, Troadec H, Wright PJ (2002) *Manual of fish sclerochronology*, Coédition
774 Ifremer-IRD.

775 Payan P, Borelli G, Boeuf G, Mayer-Gostan N (1998) Relationship between otolith and somatic
776 growth: consequence of starvation on acid-base balance in plasma and endolymph in the
777 rainbow trout *Oncorhynchus mykiss*. *Fish Physiol Biochem* 19:35–41

778 Payan P, Edeyer A, Pontual H de, Borelli G, Boeuf G, Mayer-Gostan N (1999) Chemical composition of
779 saccular endolymph and otolith in fish inner ear: lack of spatial uniformity. *Am J Physiol -*
780 *Regul Integr Comp Physiol* 277:123–131

781 Payan P, Pontual H de, Boeuf G, Mayer-Gostan N (2004) Endolymph chemistry and otolith growth in
782 fish. *Comptes Rendus Palevol* 3:535–547

783 Pisam M, Payan P, LeMoal C, Edeyer A, Boeuf G, Mayer-Gostan N (1998) Ultrastructural study of the
784 saccular epithelium of the inner ear of two teleosts, *Oncorhynchus mykiss* and *Psetta*
785 *maxima*. *Cell Tissue Res* 294:261–270

786 Post DM (2002) Using stable isotopes to estimate trophic position: models, methods, and
787 assumptions. *Ecology* 83:703–718

788 R Core Team (2014) *R: A language and environment for statistical computing*. R Foundation for
789 Statistical Computing, Vienna, Austria. URL <http://www.R-project.org/>.

790 Rohlf FJ, Archie JW (1984) A Comparison of Fourier Methods for the Description of Wing Shape in
791 Mosquitoes (Diptera: Culicidae). *Syst Biol* 33:302–317

792 Rosenblatt AE, Nifong JC, Heithaus MR, Mazzotti FJ, Cherkiss MS, Jeffery BM, Eelsey RM, Decker RA,
793 Silliman BR, Jr LJG, Lowers RH, Larson JC (2015) Factors affecting individual foraging
794 specialization and temporal diet stability across the range of a large “generalist” apex
795 predator. *Oecologia* 178:5–16

796 Sanchez-Jerez P, Gillanders BM, Kingsford MJ (2002) Spatial variability of trace elements in fish
797 otoliths: comparison with dietary items and habitat constituents in seagrass meadows. *J Fish*
798 *Biol* 61:801–821

- 799 Sasagawa T, Mugiya Y (1996) Biochemical Properties of Water-Soluble Otolith Proteins and the
800 Immunobiochemical Detection of the Proteins in Serum and Various Tissues in the Tilapia
801 *Oreochromis niloticus*. Fish Sci 62:970–976
- 802 Secor D (1992) Application of Otolith Microchemistry Analysis to Investigate Anadromy. Fish Bull
803 90:798–806
- 804 Söllner C, Burghammer M, Busch-Nentwich E, Berger J, Schwarz H, Riekel C, Nicolson T (2003) Control
805 of Crystal Size and Lattice Formation by Starmaker in Otolith Biomineralization. Science
806 302:282–286
- 807 Spitz J, Mourocq E, Schoen V, Ridoux V (2010) Proximate composition and energy content of forage
808 species from the Bay of Biscay: high- or low-quality food? ICES J Mar Sci J Cons 67:909–915
- 809 Steimle FW, Terranova RJ (1985) Energy equivalents of marine organisms from the continental shelf
810 of the temperate northwest Atlantic. J Northw Atl Fish Sci 6:117–124
- 811 Stransky C, Murta AG, Schlickeisen J, Zimmermann C (2008) Otolith shape analysis as a tool for stock
812 separation of horse mackerel (*Trachurus trachurus*) in the Northeast Atlantic and
813 Mediterranean. Fish Res 89:159–166
- 814 Suthers IM, Fraser A, Frank KT (1992) Comparison of lipid, otolith and morphometric condition
815 indices of pelagic juvenile cod *Gadus morhua* from the Canadian Atlantic. Mar Ecol Prog Ser
816 84:31–40
- 817 Svanbäck R, Persson L (2004) Individual diet specialization, niche width and population dynamics:
818 implications for trophic polymorphisms. J Anim Ecol 73:973–982
- 819 Thorrold SR, Jones CM, Campana SE (1997) Response of Otolith Microchemistry to Environmental
820 Variations Experienced by Larval and Juvenile Atlantic Croaker (*Micropogonias undulatus*).
821 Limnol Oceanogr 42:102–111
- 822 Tohse H, Saruwatari K, Kogure T, Nagasawa H, Takagi Y (2009) Control of Polymorphism and
823 Morphology of Calcium Carbonate Crystals by a Matrix Protein Aggregate in Fish Otoliths.
824 Cryst Growth Des 9:4897–4901
- 825 Tsuboi M, Gonzalez-Voyer A, Höglund J, Kolm N (2011) Ecology and mating competition influence
826 sexual dimorphism in Tanganyikan cichlids. Evol Ecol 26:171–185
- 827 Tuset VM, Rosin PL, Lombarte A (2006) Sagittal otolith shape used in the identification of fishes of
828 the genus *Serranus*. Fish Res 81:316–325
- 829 Vergara JM, López-Calero G, Robaina L, Caballero MJ, Montero D, Izquierdo MS, Aksnes A (1999)
830 Growth, feed utilization and body lipid content of gilthead seabream (*Sparus aurata*) fed
831 increasing lipid levels and fish meals of different quality. Aquaculture 179:35–44
- 832 Vignon M (2012) Ontogenetic trajectories of otolith shape during shift in habitat use: Interaction
833 between otolith growth and environment. J Exp Mar Biol Ecol 420–421:26–32
- 834 Vignon M, Morat F (2010) Environmental and genetic determinant of otolith shape revealed by a
835 non-indigenous tropical fish. Mar Ecol Prog Ser 411:231–241

- 836 Walther B, Thorrold S (2006) Water, not food, contributes the majority of strontium and barium
837 deposited in the otoliths of a marine fish. *Mar Ecol Prog Ser* 311:125–130
- 838 Ward AJW, Thomas P, Hart PJB, Krause J (2004) Correlates of boldness in three-spined sticklebacks
839 (*Gasterosteus aculeatus*). *Behav Ecol Sociobiol* 55:561–568
- 840 Worthington DG, Fowler AJ, Doherty PJ (1995) Determining the most efficient method of age
841 determination for estimating the age structure of a fish population. *Can J Fish Aquat Sci*
842 52:2320–2326
- 843
- 844

Fig. 1: Map of sampling areas in the eastern English Channel according to species. Each circle represents a fishing site and circle size gives the relative sampling abundance.

Fig. 2: Contribution of taxonomic prey categories to species specific diet, measured in terms of relative weight (%W_t, black triangle) and relative frequency of occurrence (%F_t, grey open circle).

Fig. 3: Schematic representation of the sequential steps of the four RDA statistical analyses performed to investigate the four questions of the study: (A) the global relationship between diet and otolith shape (model 1), (B) the prey categories involved in this relationship (model 2), (C) the relative contributions of diet relative composition and quantity to diet-otolith shape co-variation (model 3) and (D) the relationship between diet energy composition and otolith shape (model 4).

Fig. 4: Variation partitioning between diet and individual-state for the four questions investigated for each species. Questions investigated are organized into columns whereas species are organized into lines. Each circle corresponds to one matrix: diet matrix **D**, individual-state variable matrix **I**, diet relative composition matrix **C**, and food quantity **Q**. The number in the non-overlapping part of each circle represents the unique contribution in percentage of variation of the corresponding matrix. The number in the overlapping parts of the circles represent the joint contribution in percentage of variation of the corresponding matrices. Standard deviations obtained by bootstrapping are given for unique contributions only for ease of reading. All contributions and their standard deviations are given in Table 3 for more details. P-values of contribution fractions are indicated by the following symbols: <10%†, <5%*, <1%** , <0.1 %***.

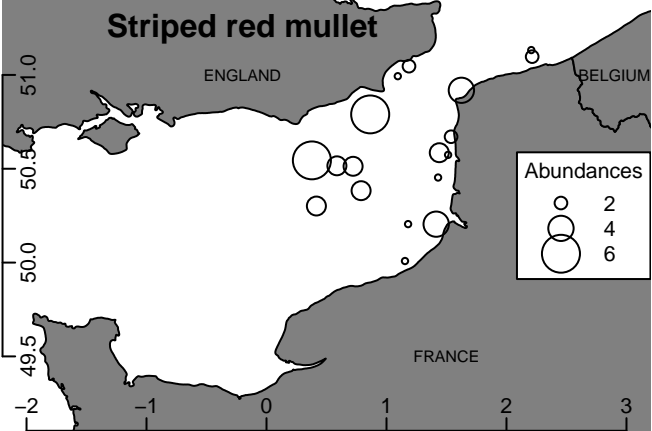
Fig. 5: pRDA biplot of otolith shape constrained by selected taxonomic prey categories and conditioned by selected individual variables (model 3) according to species. Explanatory variables with a significant effect (permutation test) on otolith shape are in red, the corresponding P-value being indicated by the following symbols: <5%*, <1%** , <0.1 %***. Each circle represents an individual and its size represents the individual total length. For each species, eight otolith shapes have been reconstructed from model predictions illustrating the relationship between diet and otolith shape.

Fig. S1: Variation partitioning between diet and individual-state for the four questions investigated for each species. Questions investigated are organized into columns whereas species are organized into lines. Each circle corresponds to one matrix: diet matrix **D**, environmental matrix **E**, individual-state variable matrix **I**, diet relative composition matrix **C**, and food quantity **Q**. The number in the non-overlapping part of each circle represents the unique contribution in percentage of variation of the corresponding matrix. The number in the overlapping parts of the circles represent the joint contribution in percentage of variation of the corresponding matrices. Standard deviations obtained by bootstrapping are given for unique contributions only for ease of reading. All contributions and their standard deviations are given in Table S5 for more details. P-values of contribution fractions are indicated by the following symbols: <10%†, <5%*, <1%** , <0.1 %***.

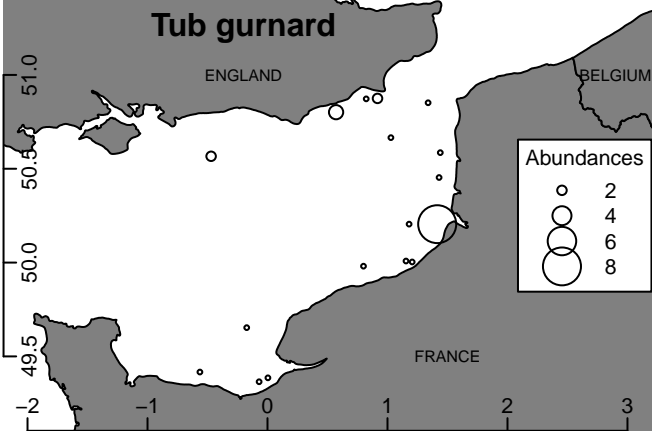
Fig. S2: pRDA biplot of otolith shape constrained by selected taxonomic prey categories and conditioned by selected individual variables and environmental variables (model 3) according to species. Explanatory variables with a significant effect (permutation test) on otolith shape are in red, the corresponding P-value being indicated by the following symbols: <5%*, <1%** , <0.1 %***. Each circle represents an individual and its size represents the individual total length. For each species, eight otolith shapes have been reconstructed from model predictions illustrating the relationship between diet and otolith shape.

Fig. S3: Contribution of energetic prey categories (● high, ● medium, ● low) to species specific diet, measured in terms of relative weight (%W_e).

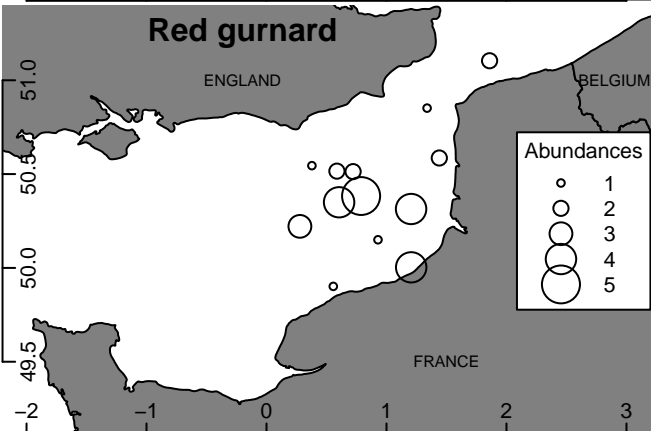
Striped red mullet



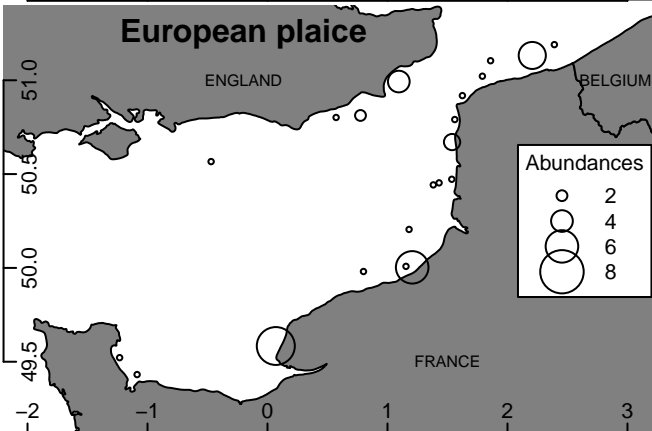
Tub gurnard



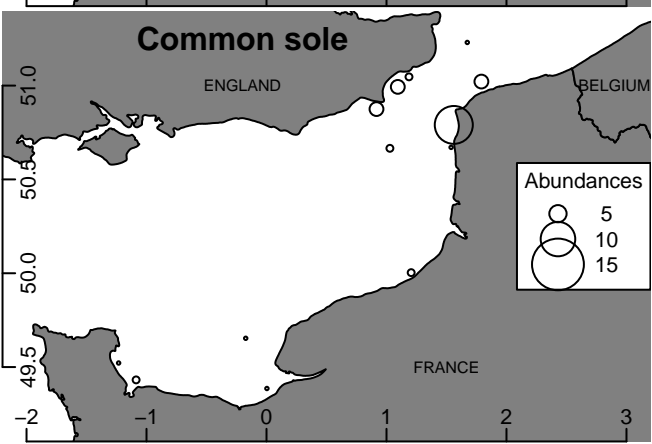
Red gurnard



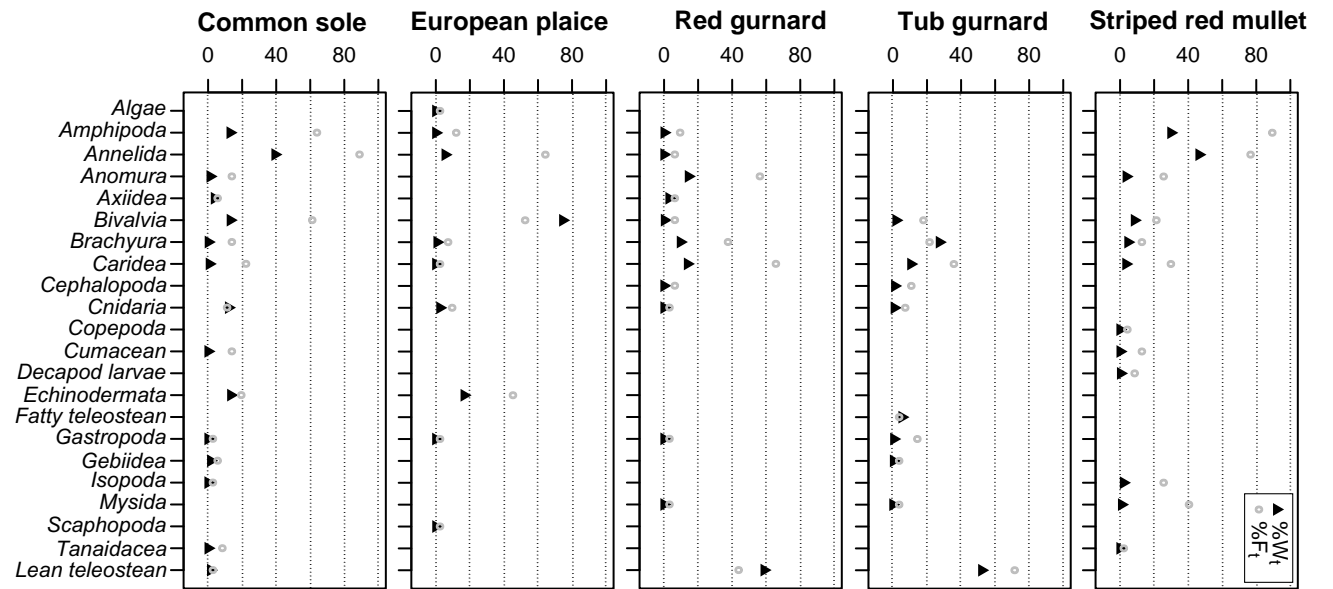
European plaice



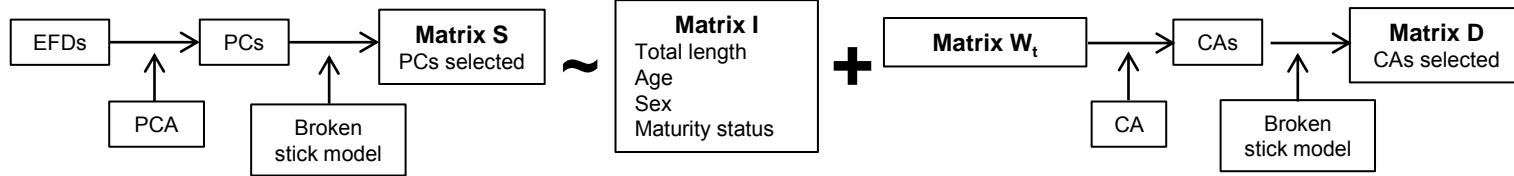
Common sole



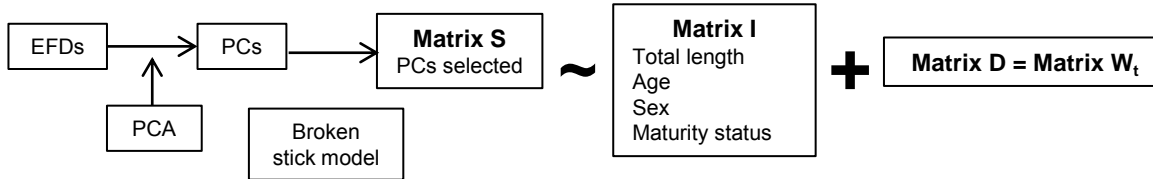
Relative weight (Wt) and relative frequency (Ft) of occurrence (%)



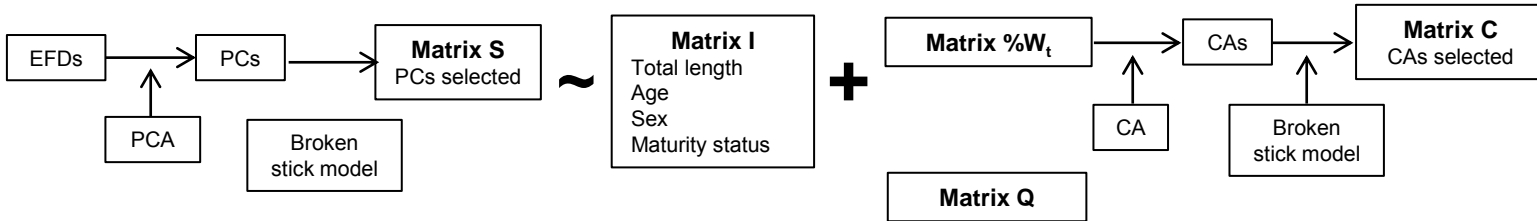
A. Global relationship between diet and otolith shape (model 1)



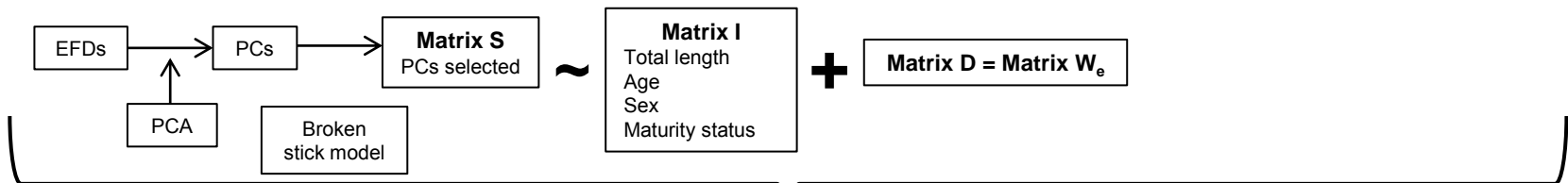
B. Taxonomic prey categories involved in the relationship between diet and otolith shape (model 2)



C. Contribution of diet relative composition vs food quantity to diet-otolith shape co-variation (model 3)



D. Relationship between diet energy composition and otolith shape (model 4)



Complete model

Stepwise selection

Selected model

Permutation tests

pRDA
&
Variance partitioning

Significance
of model

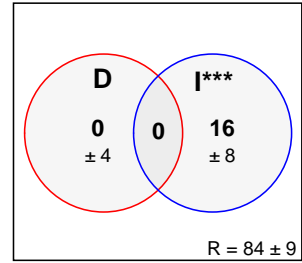
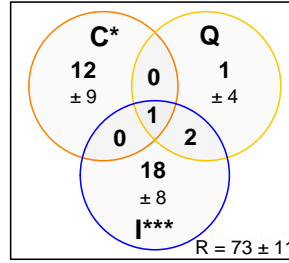
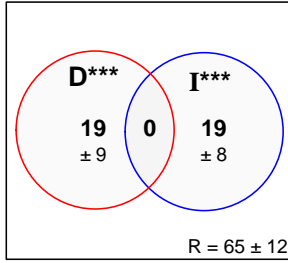
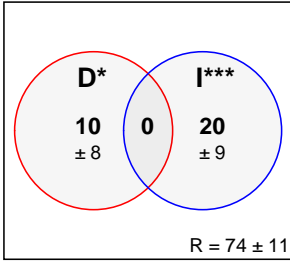
Global relationship between diet and otolith shape

Taxonomic prey categories involved in the relationship between diet and otolith shape

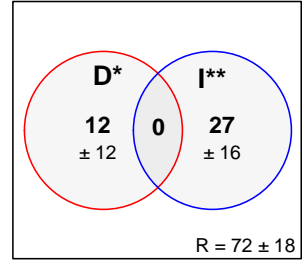
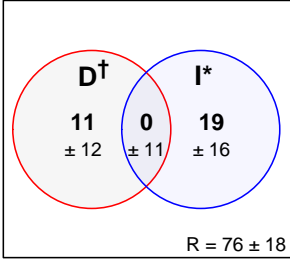
Contribution of diet relative composition vs food quantity to diet-otolith shape co-variation

Relationship between diet energy composition and otolith shape

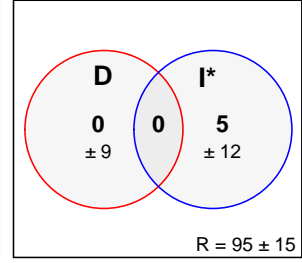
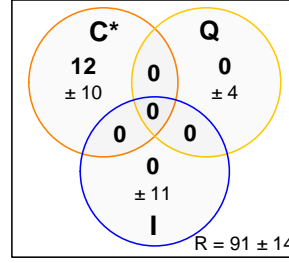
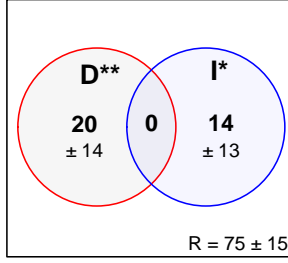
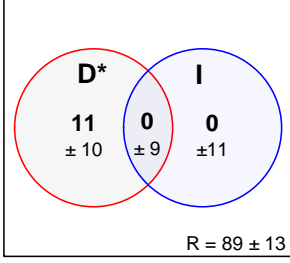
Striped red mullet



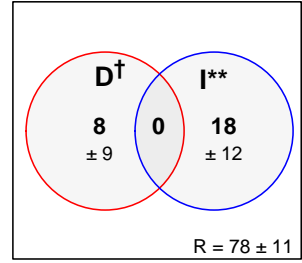
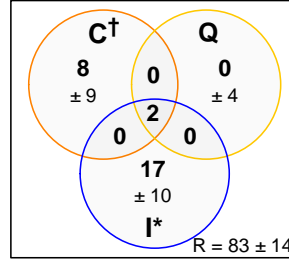
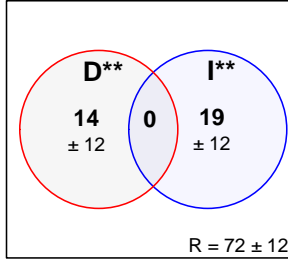
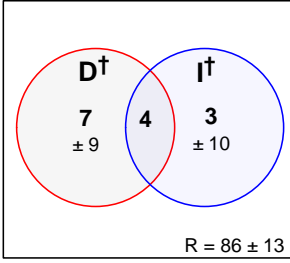
Tub gurnard



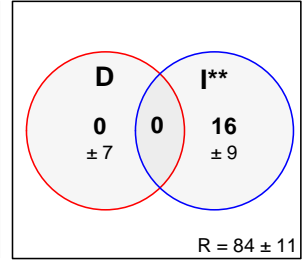
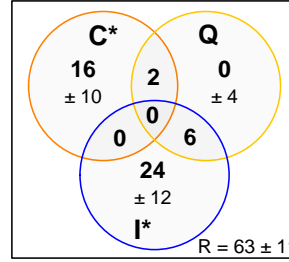
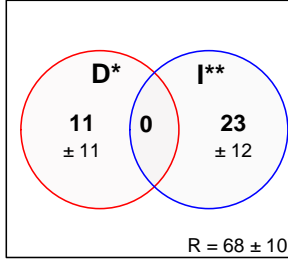
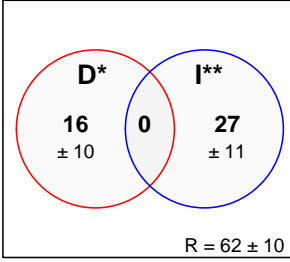
Red gurnard



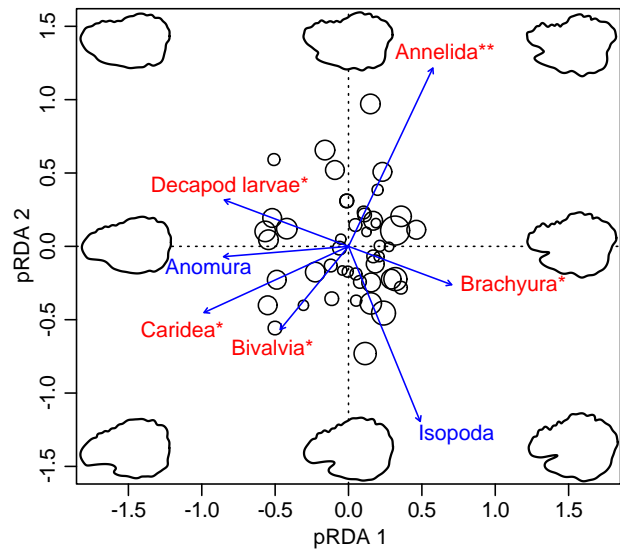
European plaice



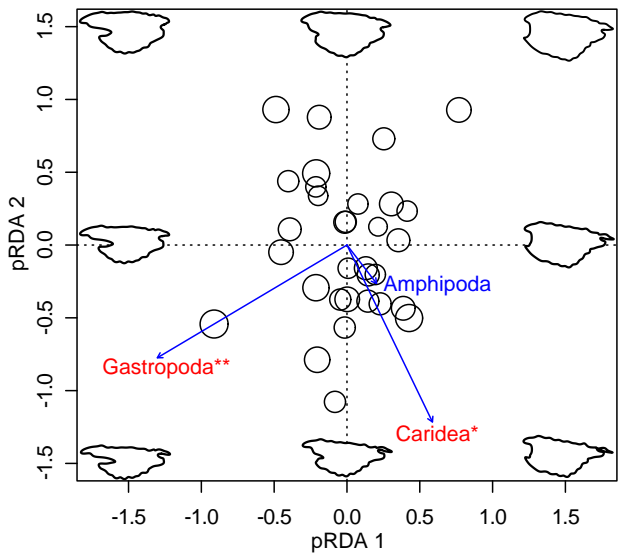
Common sole



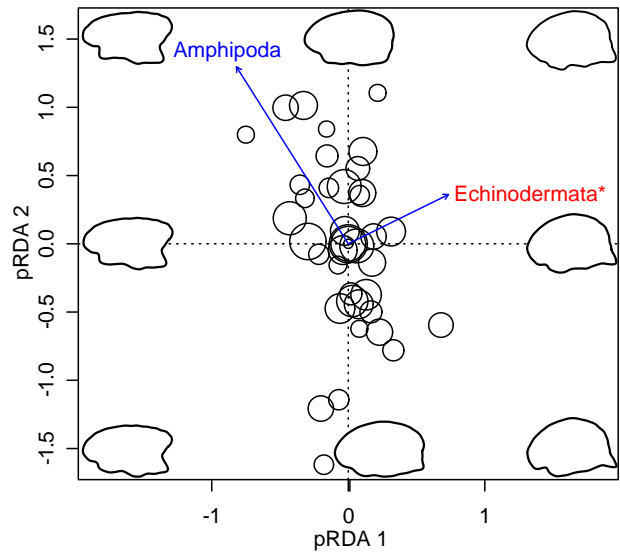
Striped red mullet



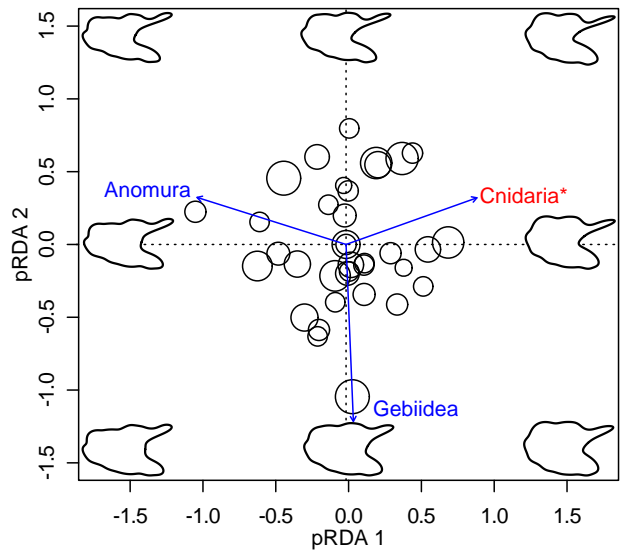
Red gurnard



European plaice



Common sole



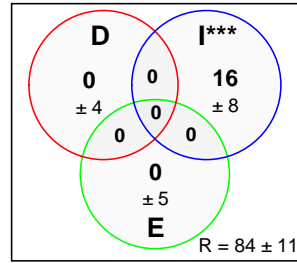
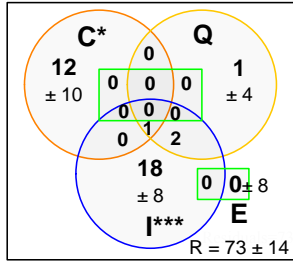
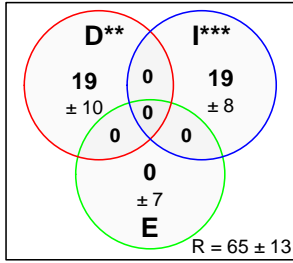
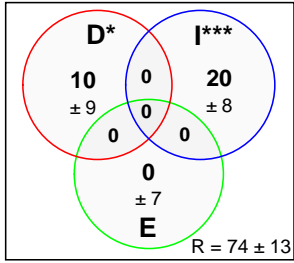
Global relationship between diet and otolith shape

Taxonomic prey categories involved in the relationship between diet and otolith shape

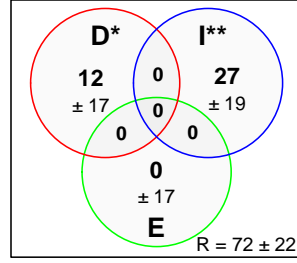
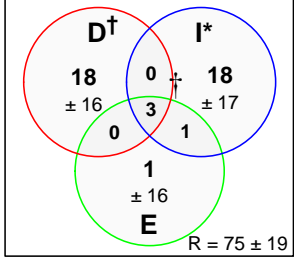
Contribution of diet relative composition vs food quantity to diet-otolith shape co-variation

Relationship between diet energy composition and otolith shape

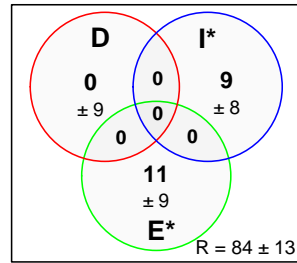
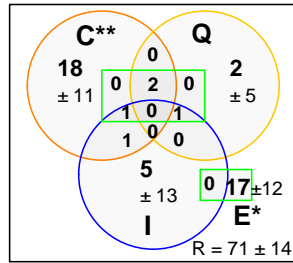
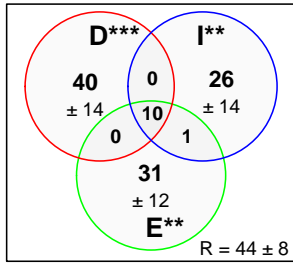
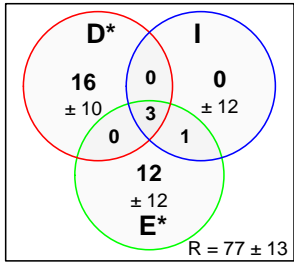
Striped red mullet



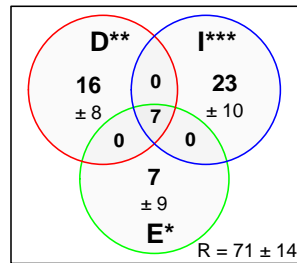
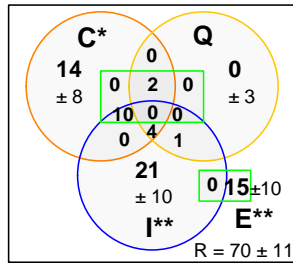
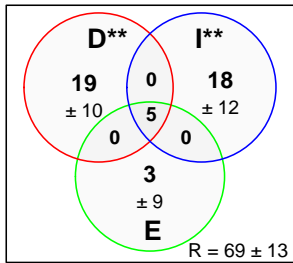
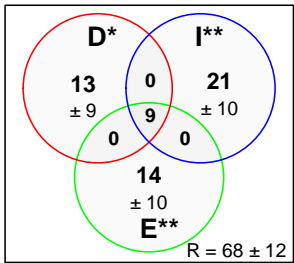
Tub gurnard



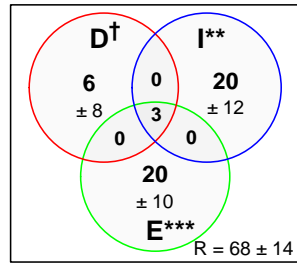
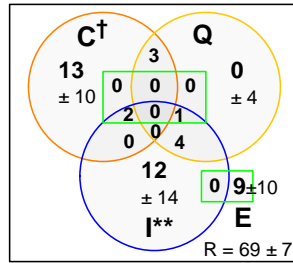
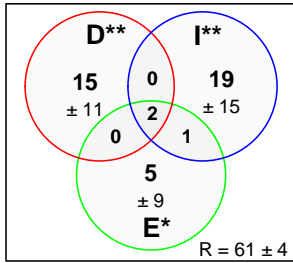
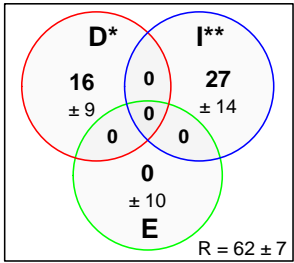
Red gurnard



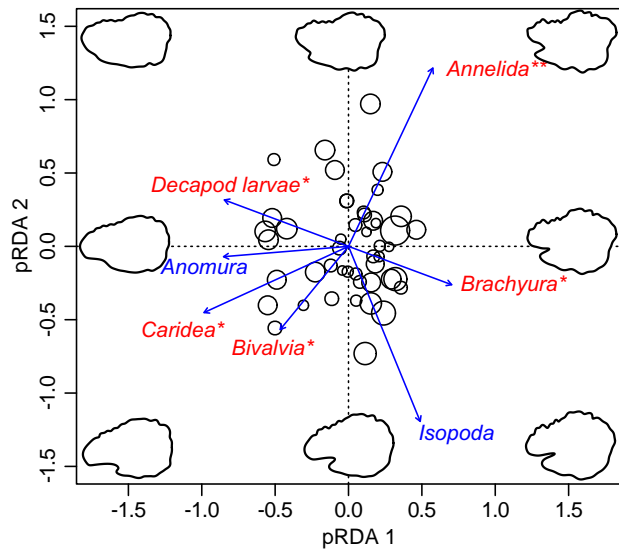
European plaice



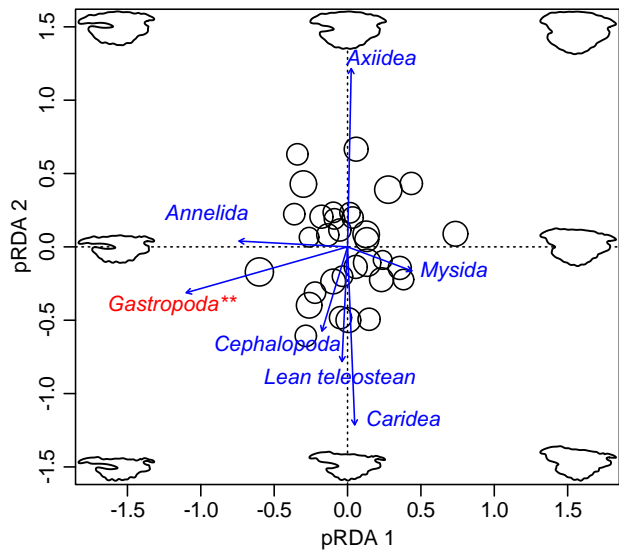
Common sole



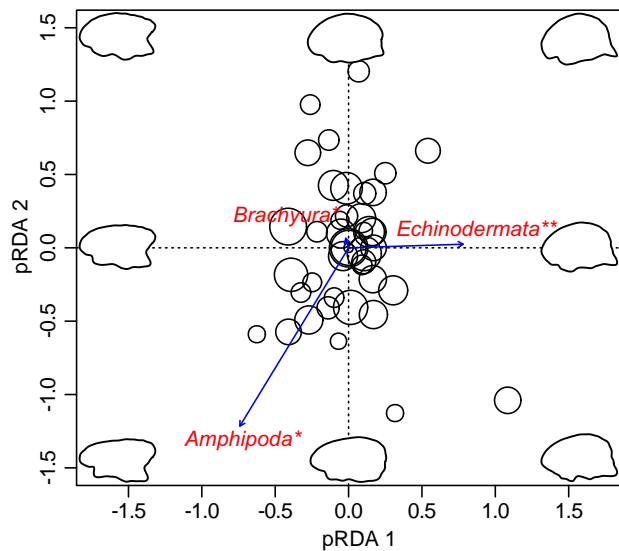
Striped red mullet



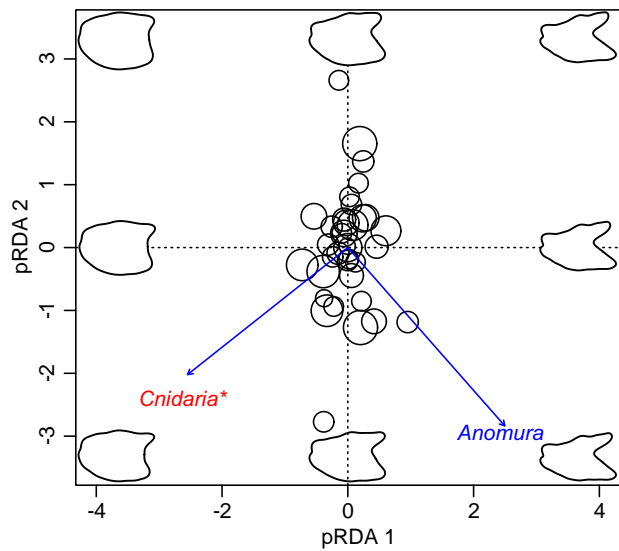
Red gurnard



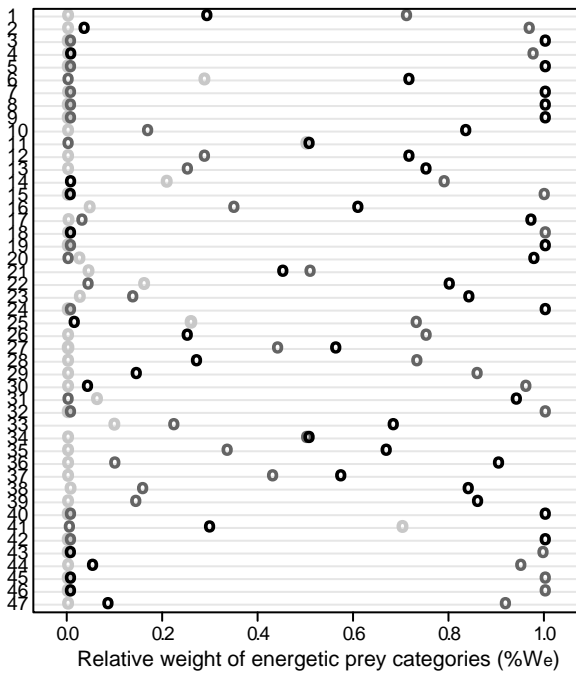
European plaice



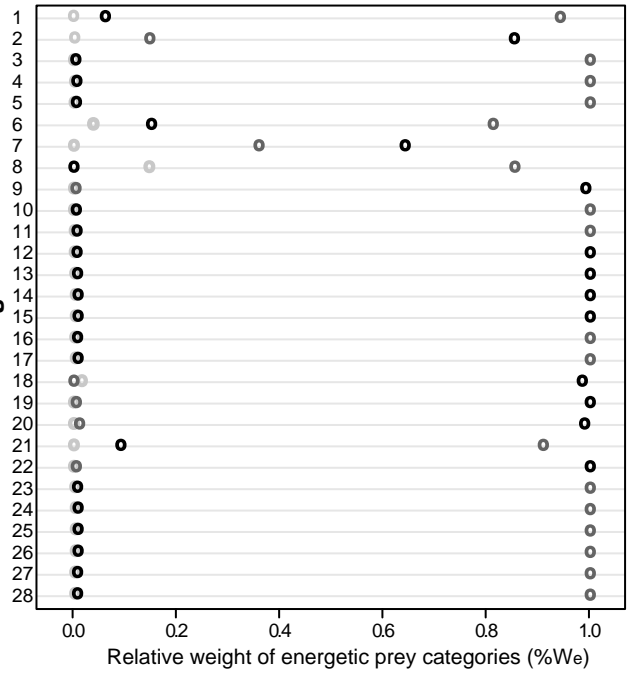
Common sole



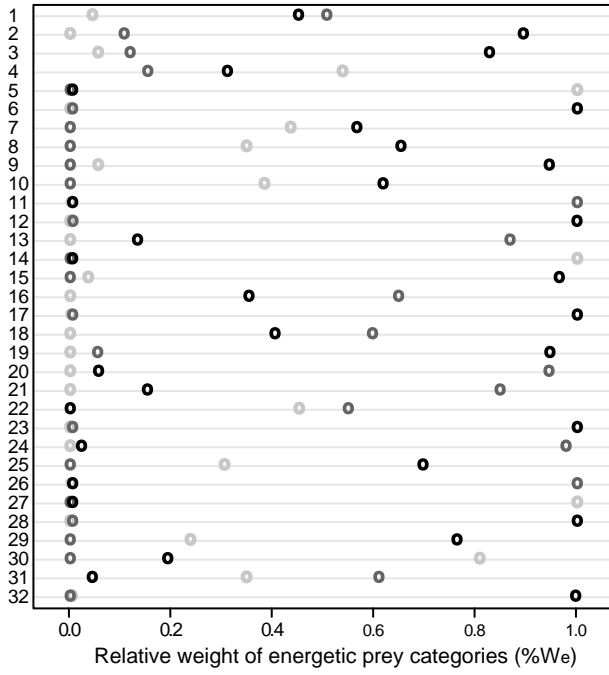
Striped red mullet



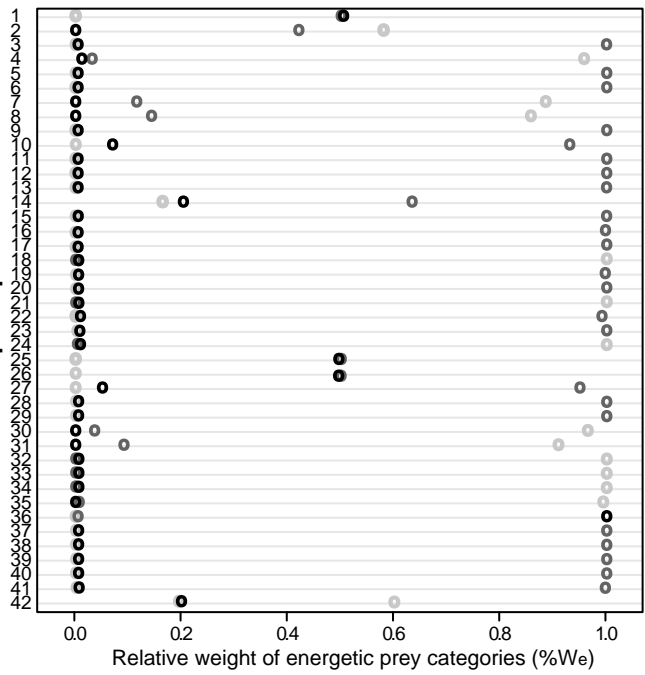
Tub gurnard



Red gurnard



European plaice



Common sole

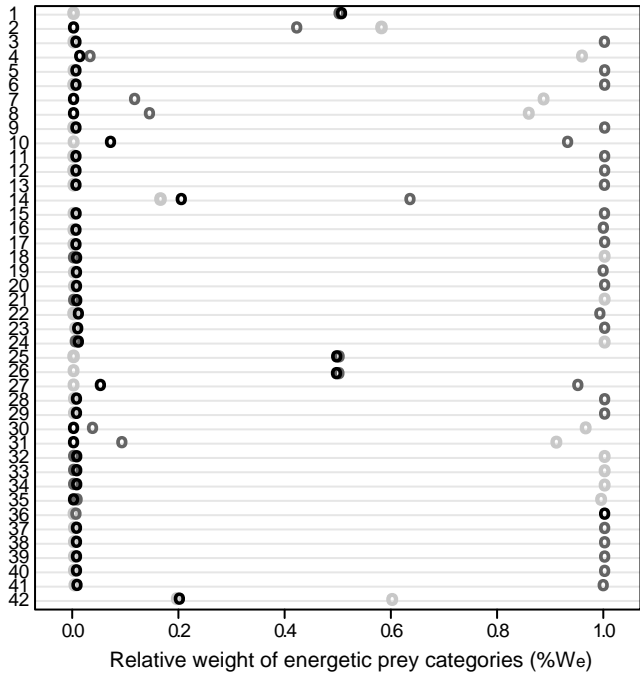


Table 1. Characteristics of the samples studied. Number of samples analyzed (N), number of females (N_F), number of males (N_M), number of individuals with undetermined sex (N_U), proportion of mature individuals (% **Mat**), age and total length distributions of the samples.

Species	N	$N_F / N_M / N_U$	% Mat	Age (years)	Total length (cm)
				Mean \pm SD Min-Max	Mean \pm SD Min-Max
Striped red mullet	47	08/16/23	48.94	0.62 \pm 0.79 0-3	16.51 \pm 5.60 9-32
Tub gurnard	28	10/18/00	32.14	1.75 \pm 0.84 0-3	25.86 \pm 6.61 16-40
Red gurnard	32	12/19/01	37.50	2.69 \pm 0.74 1-4	24.91 \pm 2.85 20-31
European plaice	42	26/14/02	76.19	1.81 \pm 1.38 0-7	27.33 \pm 7.45 9-43
Common sole	36	18/17/01	91.67	2.44 \pm 1.61 1-6	25.94 \pm 5.81 17-38

Table 2. Results of the three RDA models (as detailed in figure 3) for the five studied fish species. “Otolith shape” gives the number of principal components (N PCs) in the response matrix **S** used to describe otolith shape and the percentage of variance in Elliptical Fourier Descriptors they explain (%). “Individual” and “Diet” correspond to explanatory matrices **I**, and **D** in reduced models. More precisely, “Individual” gives the selected individual-state variables. “Diet” indicates the variables the matrix **D**, i.e. the number of correspondence axes (N CAs) and the percentage of variance they explain (%) in diet composition W_t and relative diet composition $\%W_{t,j}$ in models 1 and 3, respectively, and the selected prey categories in models 2 and 4. “Model selected” gives the degrees of freedom (df), the F statistic, the corresponding P-value and the percentage of variation explained (%) by the reduced model.

Specie	Otolith shape S		Individual I	Diet D		Model selected			
	N PCs	%		N CAs	%	df	F	P-value	%
Global relationship between diet and otolith shape (model 1)				N CAs	%				
Striped red mullet	4	77.00	Size Sex	10	99.85	13	2.22	0.002	25.61
Tub gurnard	2	70.18	Age Sex	4	90.59	8	2.06	0.016	23.95
Red gurnard	3	77.84	-	4	94.01	4	1.97	0.039	11.11
European plaice	3	74.02	Maturity	4	93.53	5	2.29	0.011	13.56
Common sole	3	78.23	Age Size Sex	8	95.32	16	2.31	0.003	37.50
Taxonomic prey categories involved in the relationship between diet and otolith shape (model 2)				Taxonomic prey category					
Striped red mullet	4	77.00	Size Sex	Annelida, Anomura, Bivalvia, Brachyura, Caridea, Decapod larvae, Isopoda		10	3.49	0.001	35.11
Tub gurnard	2	70.18	-	-		-	-	-	00.00
Red gurnard	3	77.84	Age Maturity	Amphipoda, Gastropoda, Caridea		7	2.51	0.003	25.40
European plaice	3	74.02	Age	Amphipoda, Echinodermata		8	2.94	0.004	27.51
Common sole	3	78.23	Age Size	Anomura, Cnidaria, Gebiidea		11	2.64	0.002	34.05

			Sex						
Contribution of diet relative composition vs food quantity to diet-otolith shape co-variation (model 3)				N CAs	%				
Striped red mullet	4	77.00	Size Sex	10	99.87	14	2.19	0.001	26.66
Tub gurnard	2	70.18	-	-	-	-	-	-	00.00
Red gurnard	3	77.84	-	4	94.23	5	1.61	0.012	9.02
European plaice	3	74.02	Age	4	92.64	16	2.12	0.005	30.44
Common sole	3	78.23	Age Size Sex	9	96.78	18	2.12	0.01	36.54
Relationship between diet energy composition and otolith shape (model 4)				Energetic prey category					
Striped red mullet	4	77.00	Size Sex			3	3.94	0.001	16.09
Tub gurnard	2	70.18	Age Size	low/medium/high		7	2.53	0.003	28.45
Red gurnard	3	77.84	Size			1	2.53	0.047	4.70
European plaice	3	74.02	Age	low/medium/high		9	2.27	0.014	21.76
Common sole	3	78.23	Age			5	2.38	0.007	16.43

Table 3. Percent contribution with bootstrapped standard deviation of the diet matrix (**D**), the individual matrix (**I**) and residuals (**R**), obtained from variation partitioning performed on the reduced model for the four questions investigated and each studied species

Global relationship between diet and otolith shape (model 1)								
Species	D		D&I		I		R	
Striped red mullet	10 ± 8.29		0 ± 7.31		20 ± 8.51		74 ± 10.94	
Tub gurnard	11 ± 11.73		0 ± 8.66		19 ± 15.72		76 ± 17.54	
Red gurnard	11 ± 9.71		0 ± 9.44		0 ± 11.30		89 ± 13.26	
European plaice	7 ± 9.09		4 ± 9.54		3 ± 10.18		86 ± 12.95	
Common sole	16 ± 10.28		0 ± 11.37		27 ± 11.26		62 ± 9.69	
Taxonomic prey categories involved in the relationship between diet and otolith shape (model 2)								
Species	D		D&I		I		R	
Striped red mullet	19 ± 9.30		0 ± 7.00		19 ± 8.05		65 ± 11.64	
Tub gurnard								
Red gurnard	20 ± 13.98		0 ± 15.25		14 ± 12.76		75 ± 14.52	
European plaice	14 ± 12.41		0 ± 10.29		19 ± 12.20		72 ± 11.95	
Common sole	11 ± 11.30		0 ± 14.15		23 ± 11.93		68 ± 10.12	
Contribution of diet relative composition vs food quantity to diet-otolith shape co-variation (model 3)								
Species	C	Q	I	C&Q	Q&I	C&I	C&Q&I	R
Striped red mullet	12 ± 9.46	1 ± 3.54	18 ± 7.78	0 ± 3.44	2 ± 4.89	0 ± 7.07	1 ± 5.54	73 ± 11.39
Tub gurnard								
Red gurnard	12 ± 10.04	0 ± 4.05	0 ± 11.39	0 ± 3.88	0 ± 4.31	0 ± 10.09	0 ± 4.20	91 ± 13.72
European plaice	8 ± 8.68	0 ± 3.86	17 ± 10.47	0 ± 4.45	0 ± 3.93	0 ± 10.12	2 ± 4.75	83 ± 13.53
Common sole	16 ± 10.50	0 ± 4.31	24 ± 12.10	2 ± 5.34	6 ± 6.55	0 ± 11.90	0 ± 7.05	63 ± 11.49
Relationship between diet energy composition and otolith shape (model 4)								
Species	D		D&I		I		R	
Striped red mullet	0 ± 4.34		0 ± 2.87		16 ± 7.67		84 ± 8.84	
Tub gurnard	12 ± 11.73		0 ± 8.66		27 ± 15.72		72 ± 17.54	
Red gurnard	0 ± 9.18		0 ± 7.30		5 ± 11.78		95 ± 15.01	
European plaice	8 ± 9.12		0 ± 7.68		18 ± 11.54		78 ± 11.10	
Common sole	0 ± 6.76		0 ± 5.96		16 ± 9.00		84 ± 11.08	

Table S1: Prey items found in the stomach contents of the studied species and the corresponding prey categories based on taxonomy (Taxonomic prey category) and on their energy content (Energetic prey category). References used to categorize preys in terms of energetic content are also given. When the energetic value of the prey item was not found, the energetic value of a closer taxon was used.

Prey item	Taxonomic prey category	Energetic prey category	Reference
Algae	Algae	Low	
Amphipoda	Amphipoda	High	Dauvin & Joncourt 1989 Steimle & Terranova 1985
Aphroditidae	Annelida	High	Dauvin & Joncourt 1989
Opheliidae	Annelida	High	Dauvin & Joncourt 1989
Nereidae	Annelida	High	Dauvin & Joncourt 1989
Glyceridae	Annelida	High	Dauvin & Joncourt 1989
Glycera sp	Annelida	High	Dauvin & Joncourt 1989
Phyllodocida	Annelida	High	Dauvin & Joncourt 1989
Eunicidae	Annelida	High	Dauvin & Joncourt 1989
Nephtyidae	Annelida	High	Dauvin & Joncourt 1989 Steimle & Terranova 1985
Spionidae	Annelida	Medium	Dauvin & Joncourt 1989
Chloraemidae	Annelida	Medium	Dauvin & Joncourt 1989
Pectinariidae	Annelida	Medium	Dauvin & Joncourt 1989
<i>Pectinaria koreni</i>	Annelida	Medium	Dauvin & Joncourt 1989
Terebellidae	Annelida	Medium	Dauvin & Joncourt 1989 Steimle & Terranova 1985
<i>Lanice conchilega</i>	Annelida	Medium	Dauvin & Joncourt 1989
Arenicolidae	Annelida	Medium	Dauvin & Joncourt 1989
Galatheoidea	Anomura	Low	Norrbin & Båmstedt 1984
<i>Galathea intermedia</i>	Anomura	Low	Norrbin & Båmstedt 1984
<i>Pisidia longicornis</i>	Anomura	Low	Norrbin & Båmstedt 1984
<i>Porcellana platycheles</i>	Anomura	Low	Norrbin & Båmstedt 1984
Porcellana sp	Anomura	Low	Norrbin & Båmstedt 1984
Paguroidea	Anomura	High	Dauvin & Joncourt 1989 Steimle & Terranova 1985
<i>Pagurus bernhardus</i>	Anomura	High	Dauvin & Joncourt 1989 Steimle & Terranova 1985
<i>Diogenes pugilator</i>	Anomura	High	Dauvin & Joncourt 1989 Steimle & Terranova 1985
Axiidea	Axiidea	Low	Norrbin & Båmstedt 1984
Mytilidae	Bivalvia	Medium	Dauvin & Joncourt 1989 Steimle & Terranova 1985
<i>Mytilus edulis</i>	Bivalvia	Medium	Dauvin & Joncourt 1989 Steimle & Terranova 1985
Mactridae	Bivalvia	Medium	Dauvin & Joncourt 1989 Steimle & Terranova 1985
Arcidae	Bivalvia	Medium	Dauvin & Joncourt 1989 Steimle & Terranova 1985
<i>Arca tetragona</i>	Bivalvia	Medium	Dauvin & Joncourt 1989 Steimle & Terranova 1985
Nuculidae	Bivalvia	Medium	Steimle & Terranova 1985
Nucula sp	Bivalvia	Medium	Steimle & Terranova 1985
Solenidae	Bivalvia	Medium	Dauvin & Joncourt 1989 Steimle & Terranova 1985
<i>Phaxas pellucidus</i>	Bivalvia	Medium	Dauvin & Joncourt 1989 Steimle & Terranova 1985
Ensis sp	Bivalvia	Medium	Steimle & Terranova 1985
Semelidae	Bivalvia	Medium	Dauvin & Joncourt 1989 Steimle & Terranova 1985

<i>Abra alba</i>	Bivalvia	Medium	Dauvin & Joncourt 1989
Cardiidae	Bivalvia	Medium	Dauvin & Joncourt 1989 Steimle & Terranova 1985
Parvicardium sp	Bivalvia	Medium	Dauvin & Joncourt 1989 Steimle & Terranova 1985
Solecurtidae	Bivalvia	Medium	Dauvin & Joncourt 1989 Steimle & Terranova 1985
<i>Azorinus chamasolen</i>	Bivalvia	Medium	Dauvin & Joncourt 1989 Steimle & Terranova 1985
Donacidae	Bivalvia	Medium	Dauvin & Joncourt 1989 Steimle & Terranova 1985
<i>Donax vittatus</i>	Bivalvia	Medium	Dauvin & Joncourt 1989 Steimle & Terranova 1985
Pectinidae	Bivalvia	Medium	Dauvin & Joncourt 1989 Steimle & Terranova 1985
<i>Mimachlamys varia</i>	Bivalvia	Medium	Dauvin & Joncourt 1989 Steimle & Terranova 1985
Portunidae	Brachyura	High	Spitz et al. 2010
Liocarcinus sp	Brachyura	High	Dauvin & Joncourt 1989
<i>Liocarcinus depurator</i>	Brachyura	High	Dauvin & Joncourt 1989
<i>Liocarcinus pusillus</i>	Brachyura	High	Dauvin & Joncourt 1989
Leucosiidae	Brachyura	Low	Dauvin & Joncourt 1989 Steimle & Terranova 1985
<i>Ebalia cranchii</i>	Brachyura	Low	Dauvin & Joncourt 1989 Steimle & Terranova 1985
Pinnotheridae	Brachyura	Low	Dauvin & Joncourt 1989 Steimle & Terranova 1985
<i>Pinnotheres pisum</i>	Brachyura	Low	Dauvin & Joncourt 1989
Thiinae	Brachyura	Low	Dauvin & Joncourt 1989 Steimle & Terranova 1985
<i>Thia scutellata</i>	Brachyura	Low	Dauvin & Joncourt 1989 Steimle & Terranova 1985
Atelecyclidae	Brachyura	Low	Dauvin & Joncourt 1989 Steimle & Terranova 1985
Inachidea	Brachyura	Low	Dauvin & Joncourt 1989 Steimle & Terranova 1985
<i>Macropodia rostrata</i>	Brachyura	Low	Dauvin & Joncourt 1989 Steimle & Terranova 1985
<i>Inachus dorsettensis</i>	Brachyura	Low	Dauvin & Joncourt 1989 Steimle & Terranova 1985
Crangonidae	Caridea	High	Dauvin & Joncourt 1989 Spitz et al. 2010
<i>Crangon crangon</i>	Caridea	High	Dauvin & Joncourt 1989 Spitz et al. 2010
Philocheras sp	Caridea	High	Dauvin & Joncourt 1989 Spitz et al. 2010
<i>Philocheras fasciatus</i>	Caridea	High	Dauvin & Joncourt 1989
<i>Philocheras sculptus</i>	Caridea	High	Dauvin & Joncourt 1989
<i>Philocheras trispinosus</i>	Caridea	High	Dauvin & Joncourt 1989
Hippolytidae	Caridea	High	Dauvin & Joncourt 1989 Spitz et al. 2010
Hippolyte sp	Caridea	High	Dauvin & Joncourt 1989 Spitz et al. 2010
<i>Eualus gaimardii</i>	Caridea	High	Dauvin & Joncourt 1989 Spitz et al. 2010
<i>Eualus occultus</i>	Caridea	High	Dauvin & Joncourt 1989 Spitz et al. 2010
Processidae	Caridea	High	Dauvin & Joncourt 1989 Spitz et al. 2010
Processa sp	Caridea	High	Dauvin & Joncourt 1989 Spitz et al. 2010
<i>Processa canaliculata</i>	Caridea	High	Dauvin & Joncourt 1989 Spitz et al. 2010

<i>Processa edulis</i>	Caridea	High	Dauvin & Joncourt 1989 Spitz et al. 2010
pandalidae	Caridea	High	Dauvin & Joncourt 1989 Spitz et al. 2010
<i>Pandalina brevirostris</i>	Caridea	High	Dauvin & Joncourt 1989 Spitz et al. 2010
Palaemonidae	Caridea	High	Spitz et al. 2010
Palaemon sp	Caridea	High	Spitz et al. 2010
Sepiolidae	Cephalopoda	Medium	Spitz et al. 2010
Ommastrephidae	Cephalopoda	Medium	Spitz et al. 2010
Hydrozoa	Cnidaria	Low	Steimle & Terranova 1985
Anthozoa	Cnidaria	Low	Steimle & Terranova 1985
Copepoda	Copepoda	High	Norrbin & Båmstedt 1984
Bodotriidae	Cumacean	High	Norrbin & Båmstedt 1984
Bodotria sp	Cumacean	High	Norrbin & Båmstedt 1984
<i>Bodotria arenosa</i>	Cumacean	High	Norrbin & Båmstedt 1984
<i>Bodotria scorpioides</i>	Cumacean	High	Norrbin & Båmstedt 1984
Vaunthompsonia sp	Cumacean	High	Norrbin & Båmstedt 1984
Pseudocumatidae	Cumacean	High	Norrbin & Båmstedt 1984
Pseudocuma sp	Cumacean	High	Norrbin & Båmstedt 1984
Decapod larvae	Decapod larvae	High	Norrbin & Båmstedt 1984
Echinozoa	Echinodermata	Low	Dauvin & Joncourt 1989 Steimle & Terranova 1985
<i>Echinocyamus pusillus</i>	Echinodermata	Low	Dauvin & Joncourt 1989 Steimle & Terranova 1985
Asterozoa	Echinodermata	Low	Dauvin & Joncourt 1989 Steimle & Terranova 1985
<i>Ophiutrix fragilis</i>	Echinodermata	Low	Dauvin & Joncourt 1989 Steimle & Terranova 1985
Ophiuridae	Echinodermata	Low	Dauvin & Joncourt 1989
<i>Mullus surmuletus</i>	Fatty teleostean	High	Spitz et al. 2010
<i>Trachurus Trachurus</i>	Fatty teleostean	High	Spitz et al. 2010
Naticidae	Gastropoda	Medium	Dauvin & Joncourt 1989
Euspira sp	Gastropoda	Medium	Dauvin & Joncourt 1989
Lacunidae	Gastropoda	Medium	Dauvin & Joncourt 1989
Littorinidae	Gastropoda	Medium	Dauvin & Joncourt 1989
Calyptraeidae	Gastropoda	Medium	Dauvin & Joncourt 1989
<i>Crepidula fornicata</i>	Gastropoda	Medium	Dauvin & Joncourt 1989
Buccinidae	Gastropoda	Medium	Dauvin & Joncourt 1989
Gebiidea	Gebiidea	High	Norrbin & Båmstedt 1984
Isopoda	Isopoda	High	Dauvin & Joncourt 1989
Mysida	Mysida	High	Norrbin & Båmstedt 1984
Scaphopoda	Scaphopoda	High	Dauvin & Joncourt 1989
<i>Upogebia deltaura</i>	Tanaidacea	High	Dauvin & Joncourt 1989
Perciformes	Lean teleostean	Medium	Spitz et al. 2010
<i>Callionymus lyra</i>	Lean teleostean	Medium	Spitz et al. 2010
Gobiidae	Lean teleostean	Medium	Spitz et al. 2010
Pleuronctiformes	Lean teleostean	Medium	Spitz et al. 2010
<i>Solea Solea</i>	Lean teleostean	Medium	Spitz et al. 2010

Table S2. Results of the four RDA models (as detailed in figure 3) for the five studied fish species. “Otolith shape” gives the number of principal components (N PCs) in the response matrix **S** used to describe otolith shape and the percentage of variance in Elliptical Fourier Descriptors they explain (%). “Environment”, “Individual” and “Diet” correspond to explanatory matrices **E**, **I**, and **D** in reduced models. More precisely, “Environment” and “Individual” give the selected environmental and individual-state variables, respectively. “Diet” indicates the variables in the matrix **D**, i.e. the number of correspondence axes (N CAs) and the percentage of variance they explain (%) in diet composition W_t and relative diet composition $\%W_{t,j}$ in models 1 and 3, respectively, and the selected prey categories in models 2 and 4. “Model selected” gives the degrees of freedom (df), the F statistic, the corresponding P-value and the percentage of variation explained (%) by the reduced model.

Species	Otolith shape S		Environment E	Individual I	Diet D		Model selected			
	N PCs	%			N CAs	%	df	F	P-value	%
Global relationship between diet and otolith shape (model 1)					N CAs	%				
Striped red mullet	4	77	-	Size Sex	10	99.85	13	2.22	0.001	25.61
Tub gurnard	2	70.18	Longitude×Latitude	Age Sex	4	90.59	11	1.83	0.041	25.31
Red gurnard	3	77.84	Longitude×Latitude Temperature		4	94.01	8	2.15	0.007	22.89
European plaice	3	74.02	Temperature Salinity	Age Sex Maturity	4	93.53	15	2.28	0.001	31.94
Common sole	3	78.23	-	Age Size Sex	8	95.32	16	2.31	0.003	37.50
Taxonomic prey categories involved in the relationship between diet and otolith shape (model 2)					Taxonomic prey category					
Striped red mullet	4	77	-	Size Sex	Annelida, Anomura, Bivalvia, Brachyura, Caridea, Decapod larvae, Isopoda		10	3.49	0.001	35.11
Tub gurnard	2	70.18	-	-	-	-	-	-	-	00.00
Red gurnard	3	77.84	Longitude×Latitude Temperature Depth	Size Age Maturity	Annelida, Axiidea, Caridea, Cephalopoda,		17	3.28	0.001	55.56

					Gastropoda, Mysida, Teleostean					
European plaice	3	74.02	Depth	Age	Amphipoda, Brachyura, Echinodermata	10	2.85	0.001	31.10	
Common sole	3	78.23	Temperature	Age Size Sex	Anomura, Caridea, Cnidaria	12	2.85	0.001	38.85	
Contribution of diet relative composition vs food quantity to diet-otolith shape co-variation (model 3)					N	CAs	%			
Striped red mullet	4	77	-	Size Sex	10	99.87	14	2.19	0.001	26.66
Tub gurnard	2	70.18	-	-	-	-	-	-	-	00.00
Red gurnard	3	77.84	Longitude×Latitude Temperature	Maturity	4	94.23	10	2.24	0.004	28.63
European plaice	3	74.02	Temperature Salinity	Age Sex Maturity	4	92.64	16	2.12	0.005	30.44
Common sole	3	78.23	Temperature Longitude×Latitude	Size	9	96.78	15	2.04	0.002	30.77
Relationship between diet energy composition and otolith shape (model 4)					Energetic prey category					
Striped red mullet	4	77	-	Size Sex			3	3.94	0.001	16.09
Tub gurnard	2	70.18	-	Age Size	low/medium/high		7	2.53	0.003	28.45
Red gurnard	3	77.84	Longitude×Latitude	Size			4	2.41	0.006	15.43
European plaice	3	74.02	Salinity Depth	Age	low/medium/high		11	2.51	0.004	28.80
Common sole	3	78.23	Temperature Longitude×Latitude Depth	Size Sex	low/medium/high		11	2.51	0.001	32.20

Table S3. Individual-state (*A* : age, *L_T* : total length, *Se* : sex, *M* : maturity) variables acting on otolith shape according to the model and the species considered. For each effect kept in the model reduced by stepwise selection, the *F* statistic (while respecting marginality of the effects, type 2 tests) is given together with the numerator degrees of freedom as exponent and the denominator degrees of freedom as index. The corresponding *P*-value is indicated by the following symbols: <5%*, <1%** , <0.1 %***.

Species	<i>A</i>	<i>L_T</i>	<i>Se</i>	<i>M</i>
Global relationship between diet and otolith shape (model 1)				
Striped red mullet		2.98 ¹ ₃₃ *	4.46 ² ₃₃ ***	
Tub gurnard	2.64 ³ ₁₈ *		5.67 ¹ ₁₈	
Red gurnard				
European plaice	2.11 ⁶ ₂₆ *		3.00 ² ₂₆ *	2.40 ¹ ₂₆
Common sole	2.30 ⁵ ₁₉ *	2.87 ¹ ₁₉ *	2.45 ² ₁₉ *	
Prey categories involved in the relationship (model 2)				
Striped red mullet		4.41 ¹ ₃₆ *	4.41 ² ₃₆ ***	
Tub gurnard				
Red gurnard	1.30 ³ ₁₆	0.17 ¹ ₁₆		2.54 ¹ ₁₆
European plaice	2.65 ⁶ ₃₁ **			
Common sole	1.62 ⁵ ₂₆	3.13 ¹ ₂₆ *		
Contribution of diet relative composition VS food quantity (model 3)				
Striped red mullet		3.80 ¹ ₃₂ **	4.38 ² ₃₂ ***	
Tub gurnard				
Red gurnard				1.98 ¹ ₂₃
European plaice	2.02 ⁶ ₂₅ *		3.01 ² ₂₅ *	2.58 ¹ ₂₅
Common sole		3.87 ¹ ₂₂ *		
Relationship between diet energy composition and otolith shape (model 4)				
Striped red mullet		3.47 ¹ ₄₃ *	2.68 ² ₄₃ **	
Tub gurnard	3.40 ³ ₂₀ **	4.03 ¹ ₂₀ *		
Red gurnard		2.53 ¹ ₃₀ *		
European plaice	2.42 ⁶ ₃₂ *			
Common sole	2.38 ⁵ ₃₀ **			